WVT-TR-75043

AD

12

CANNON MUZZLE BLAST NOISE SUPPRESSION FACILITY

July 1975

BENET WEAPONS LABORATORY
WATERVLIET ARSENAL
WATERVLIET, N.Y. 12189

TECHNICAL REPORT

AMCMS No. 662603.11.H7800

Pron No. M7-5-R0082-02-M7-M7

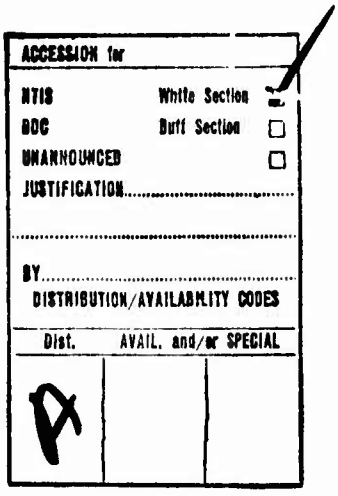

DISPOSITION

Destroy this report when it is no longer needed. Do not return it to the originator.

DISCLAIMER

The findings in this report are not to be construed as an official Department of the Army position unless so designated by other authorized documents.

UNCLASSIFIED

SECURITY CLASSIFICATION OF THIS PAGE (When Data Entered)

REPORT DOCUMENTATION PAGE

READ INSTRUCTIONS BEFORE COMPLETING FORM

1. REPORT NUMBER (14) WVT-TR-75043 | 2. GOVT ACCESSION NO. | 3. RECIPIENT'S CATALOG NUMBER

4. TITLE (and Subtitle)

(6) CANNON MUZZLE BLAST NOISE SUPPRESSION FACILITY.

5. TYPE OF REPORT & PERIOD COVERED

6. PERFORMING ORG. REPORT NUMBER

7. AUTHOR(s)

(10) H. J. SNECK

8. CONTRACT OR GRANT NUMBER(s)

9. PERFORMING ORGANIZATION NAME AND ADDRESS

Benet Weapons Laboratory
Watervliet Arsenal, Watervliet, N.Y. 12189
SARWV-RT

10. PROGRAM ELEMENT, PROJECT, TASK AREA & WORK UNIT NUMBERS

~~AMCMS 662605.11.H7800~~
(16) Proj [redacted] M7-5-R0082-02-M7-M7

11. CONTROLLING OFFICE NAME AND ADDRESS

U.S. Army Armament Command
Rock Island, Illinois 61201

12. REPORT DATE

(11) Jul[redacted]75

13. NUMBER OF PAGES

60

14. MONITORING AGENCY NAME & ADDRESS (if different from Controlling Office)

(9) Technical rept.

15. SECURITY CLASS. (of this report)

UNCLASSIFIED

15a. DECLASSIFICATION/DOWNGRADING SCHEDULE

16. DISTRIBUTION STATEMENT (of this Report)

Approved for public release; distribution unlimited.

(12) 63p.

17. DISTRIBUTION STATEMENT (of the abstract entered in Block 20, if different from Report)

18. SUPPLEMENTARY NOTES

19. KEY WORDS (Continue on reverse side if necessary and identify by block number)

Noise Reduction	Gas Flow
Blast	Acoustic Flow Theory
Fluid Mechanics	Suppressors
Dense Gases	Design

20. ABSTRACT (Continue on reverse side if necessary and identify by block number)

This report describes the theoretical and analytical investigation of a stationary noise suppressor for cannons.

A water table model was used to establish the basic suppressor configuration.

Shock wave and lumped parameter mathematical models were used to analyze suppressor performance.

DD FORM 1 JAN 73 1473 EDITION OF 1 NOV 65 IS OBSOLETE

371 075

UNCLASSIFIED

SECURITY CLASSIFICATION OF THIS PAGE (When Data Entered)

20.

(3.) A model 20mm suppressor was constructed, ~~and~~ tested, and

(4.) The calculated performance of the 20mm suppressor was found to compare favorably with test results.

(5.) A full scale suppressor (for 155mm gun) was designed on the basis of analysis and model tests;

(6.) A simplified version ~~of the full scale design~~ was constructed and field tested.

(7.) The simplified full scale suppressor successfully reduced the noise levels to acceptable values.

WVT-TR-75043

AD

CANNON MUZZLE BLAST NOISE SUPPRESSION FACILITY

H. J. Sneck

July 1975

BENET WEAPONS LABORATORY
WATERVLIET ARSENAL
WATERVLIET, N.Y. 12189

TECHNICAL REPORT

AMCMS No. 662603.11.H7800

Pron No. M7-5-R0082-02-M7-M7

TABLE OF CONTENTS

FIGURES

GLOSSARY OF TERMS

$A_{1,2,3}$ = cross-sectional area of suppressor expansion chamber

A_b = area of hemisphere having diameter of projectile

A_0 = cross-sectional area of orifice

C = sound speed

Cv_0 = ambient air specfic heat

Cv_m = combustion products specific heat

d = orifice diameter

d_p = projectile diameter

D = chamber diameter

E = internal energy ratio

f = frequency

F = Fourier transform

h = height of gun above ground plane

$$K = \left(\frac{2}{\gamma_m + 1}\right)^{\frac{\gamma_m + 1}{2(\gamma_m - 1)}} A_o \sqrt{\frac{\gamma_m g_o}{R}}$$

L = projectile length

m = mass flow rate

M_{so} = shock Mach number of blast wave generated by barrel uncorking relative to moving gas

$M_s = M_{so} + M_p$ = muzzle blast wave Mach number relative to ground

$M_{1,2,3}$ = Mach number of shock waves in expansion chambers

M_p = projectile Mach number

P_s = shock wave pressure

P_b = barrel uncorking pressure

P_0 = ambient pressure

P_{s0} = shock wave pressure generated by barrel uncorking

$P_{1,2,3}$ = pressure in expansion chambers

$\hat{P}_p$ = projectile shock wave overpressure

$P_{R1,2,3}$ = reflected pressures at baffles

$\hat{P}$ = muzzle blast wave overpressure

$\hat{P}(r)$ = overpressure at radial distance r from orifice

$\hat{P}(R)$ = overpressure at orifice

$\Delta P_{R1,2,3}$ = maximum pressure difference across baffle

r = radial distance from suppressor exit orifices

$\mathcal{R}$ = gas constnat

R = radius of orifice baffle

SPL = sound pressure level

t = time

t_o = muzzle blast wave time constnat

t_b = barrel discharge time constant

$T_{1,2,3}$ = chamber gas temperatures

T = N-wave period

T_b = gas temperature in barrel when uncorked

T_0 = ambient gas temperature

v_p = projectile velocity

v_b = muzzle blast wave velocity

v_s = projectile shock wave velocity

V_b = barrel volume

$V_{1,2,3}$ = chamber volume

y = distance measured normal to projectile path

α = projectile shock wave angle

$$\alpha_o = \frac{\gamma_m + 1}{\gamma_m - 1}$$

$$\beta = \frac{\gamma_m - 1}{2\gamma_m}$$

γ_o = ambient air specific heat ratio

γ_m = combustion products specific heat ratio

$$\mu = \frac{\gamma_o - 1}{\gamma_o + 1}$$

ρ = chamber gas density

$\dot{\rho}$ = time rate of gas density change

ρ_a = ambient air density

$\hat{\rho}$ = over-density

ρ_b = barrel gas density

$\hat{\rho}_m$ = maximum barrel over-density

$$\tau = \frac{T}{2}$$

τ_o = ratio of first chamber volume to barrel volume

τ_{12} = "time constant" for first baffle

τ_{23} = "time constant" for second baffle

$\tau_{1,2,3}$ = chamber time constants

ω = angular frequency

INTRODUCTION

With the advent of a greater awareness regarding the quality of our environment we have witnessed a growing concern about a long neglected aspect of that environment, man-made noise. In the not too distant past the general public tolerated noise as a necessary by-product of an industrialized society. In many instances, it still associates and demands noise as a sensory component of an activity, i.e., auto-racing, spectator sports, and fireworks.

In the future, however, the public through its governmental regulatory agencies will insist that unwanted sound be reduced to the lowest levels which are technically feasible. If these are still not tolerable public pressure followed by legal measures may then force the cessation of the noise producing activity altogether.

The regular or even sporadic sound of cannon fire obviously does not fall into the category of desirable out-of-doors sound to many people. In the field of human relations it is a well-known fact that an aroused, vocal minority is all that is necessary to initiate profound changes which affect all. Experience has shown that this is certainly the case with regard to the problem at hand.

Although a forthright and consistant public relations policy is certainly helpful in mitigating some of its effects, there is obviously no substitute for curing the problem at its source. Actually there are two aspects to the "cure". One is the reduction of the sound

level generated at the source, and the other is the control of its transmission through the atmosphere to the listener. Much has been written concerning the latter problem, and much remains to be learned. Relatively little has been done about the former problem, i.e., the control of the noise generated at the source. What follows is at least a beginning in that direction.

I. WATER TABLE MODELING OF THE SUPPRESSOR

It was obvious from the outset of this project that the design of a device which would successfully suppress the noise generated by a cannon's muzzle blast could not be based on the established techniques which are employed to design conventional sound suppressors. For one thing, the sound to be attenuated is non-periodic and transient rather than periodic and steady. As a consequence, the signal to be attenuated contains the complete spectrum of frequencies rather than the discrete, finite, set found in periodic signals. Fortunately, this difference does not prove to be particularly troublesome, a point which will be demonstrated analytically later in the report

Even more important than the difference in frequency content is the relative amplitude of the pressure signal to be processed. Conventional mufflers are designed to attenuate pressure signals which are measured in fractions of the ambient pressure, i.e., signals which classify as acoustic pressure waves. The pressure disturbance produced at the muzzle of a cannon is measured in tens of atmospheres and therefore causes extremely strong shock waves to propagate away from the muzzle in the vicinity of the muzzle. As a consequence, instead of small pressure perturbations superposed upon a steady bulk flow, a cannon blast-suppressor is subjected to large pressure fluctuations (and flow fluctuations) superposed upon the quiescent ambient and its relatively small absolute pressure. In addition to the obvious threat to structural integrity such pressures pose, the unsteady propagation of strong shock waves within the suppressor do not conform to classical concepts of pressure wave transmission through acoustic mufflers.

The realization that the design of a transient, high pressure-shock wave attenuator would require exploring untrod ground led to the decision to "model" the transient flow behavior on a water table before attempting any analytical description of the flow. The intent of the water table experiments was to simulate the flow conditions within the suppressor over a time scale which was much longer than the actual firing time for a cannon. This change of time scale allowed the visual observation of the sequence of events which occur within the suppressor when the barrel gases are uncorked by the projectile. Unfortunately, there is no known way to quantitatively translate the water table flow measurements into three-dimensional gas flow predictions. Nevertheless, the observed behavior of various suppressor designs on the water table did provide a valuable qualitative insight into the effectiveness of various trial configuration. Because of the rapidity with which designs can be altered and tested on the table it was possible to pursue an iterative design sequence toward the ultimate goal of maximizing the blast signal attenuation, while minimizing the internal pressures exerted on the suppressor structure.

After many unsuccessful tries the arrangement shown in Figure 1 illustrates what was finally considered to be a reasonable resolution of the overall problem. Many arrangements of baffle spacing and suppressor outer envelope size were found to be effective in considerably reducing the size of the shock wave emitted by the suppresssor relative to the size of the wave impressed on it by the discharging barrel. Given a sufficient number of baffles with orifices not much larger than the barrel bore, it was found that the original shock wave formed at the

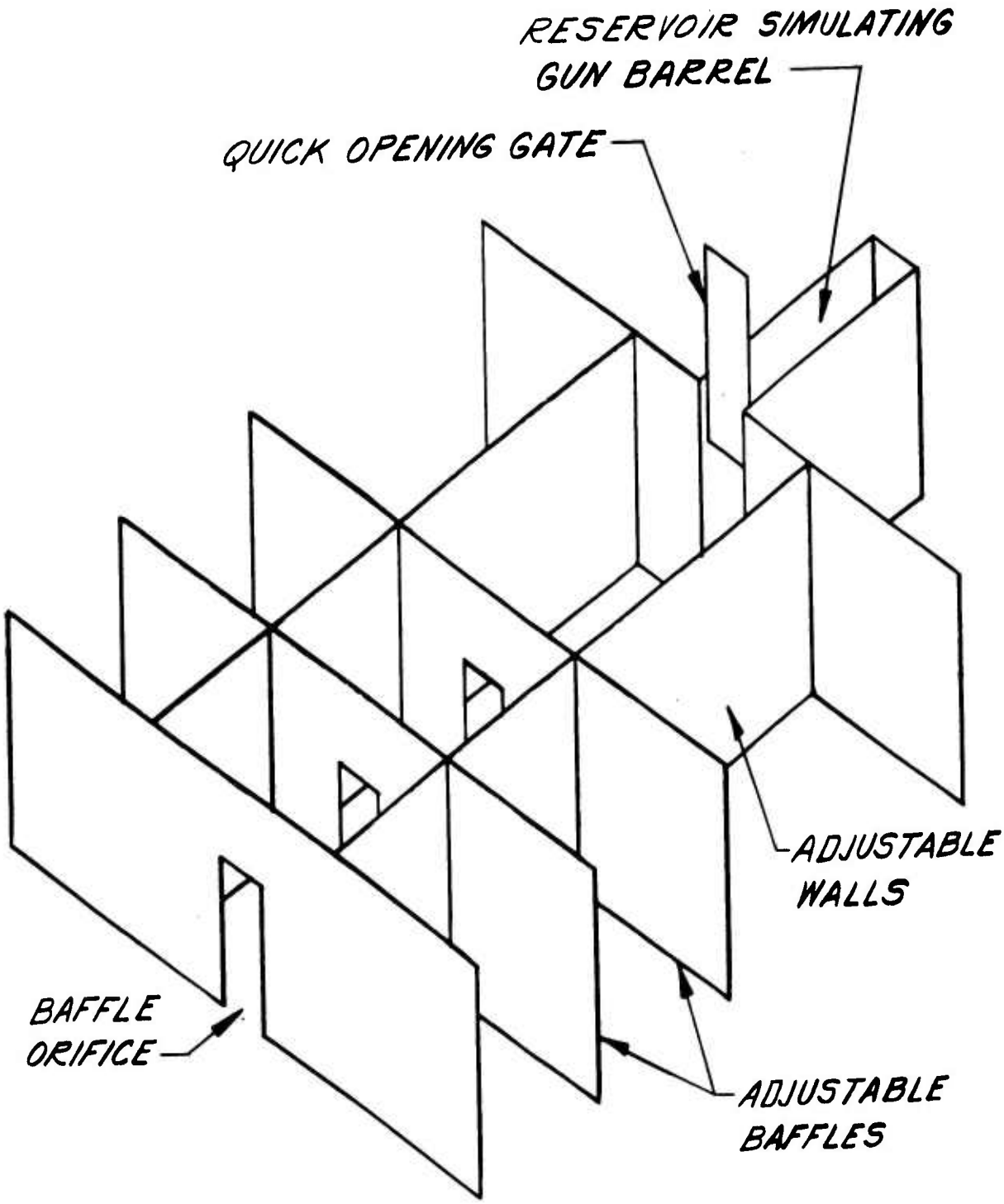

Figure 1. Water table model.

muzzle could always be reduced to what could be considered the acoustical level at the suppressor outlet. As a practical matter, three or four baffles were usually sufficient to meet this requirement.

On the other hand, if the outer envelope of the suppressor was kept to a reasonable size it was never possible to reduce the reflected internal pressures on the side walls and the baffle at the end of the first chamber to what could be considered reasonable levels. It soon became apparent that no matter how far away from the muzzle the first baffle was placed (within reason, of course) the side walls of the suppressor would always channel an undiminished shock wave the entire length of the first chamber where its full strength would impinge on the first baffle. No arrangement of partial baffles, deflectors or other impediments was found effective in reducing the large reflected pressure caused by this initial strong shock wave. Visual evidence of the destructiveness of this shock wave is presented in Reference 1 which describes the testing of a full-scale suppressor for an M-68 cannon. This suppressor eventually succumbed to an internal structural failure in which the first baffle suffered a severe "dishing", apparently caused by the impulsive force of this initial shock wave.

Having failed to eliminate this potentially destructive shock wave it became clear that it would have to be contained within the silencer itself. From a structural point of view, this could best be done by

---

[1]W.E. Page and J.V. Conners, "The Feasibility of Silencing the M68 Cannon Using an Experimental Artillery Silencer" Re 69-1985

M.J. Salsbury, "Feasibility of an Artillery Silencer" 69-1632, both from USAWC, R&D Directorate Artillery Systems Laboratory

confining the initial blast to a small, very strong chamber (or chambers) which form what amounts to a high pressure pre-suppressor contained within the envelope of the suppressor proper. The function of this pre-suppressor is to strongly attenuate the initial shock wave to a level where the wave released by it into the structurally weaker, larger, chamber would not produce large reflected pressures on its end baffle and side walls.

Simulations on the water table indicated that the pre-suppressor would indeed have to be a very strong vessel to withstand the expected muzzle shock-wave pressures. It was felt, however, that sufficiently strong vessels could be fabricated provided that they were small. The water table tests also revealed that even though a relatively strong shock wave issued from the pre-suppressor, the reflected pressures it produced on the first large chamber walls and baffle were greatly reduced relative to those found in the more conventional design.

Thus, at the end of the water table simulation phase the first objectives of the project had been reached, i.e., to determine the general fluid-mechanic behavior of suppressors subjected to pulsed inputs, the potential structural problems associated with the fluid flow, and the establishment of a preliminary design concept.

II. BLAST WAVE ANALYSIS OF 20MM SUPPRESSOR DESIGN

At this point it was decided that before launching into the design, construction, and testing of a full-scale suppressor for the larger guns, it would be wise to perform some field tests on a model suppressor using a small caliber cannon. In this way the validity of the general design

concepts which evolved from the water table tests could be determined. In addition, the analytical techniques proposed for predicting the suppressor's attenuation characteristics could also be evaluated. Should they prove to be reasonable correct, these techniques would prove a means of scaling the model test results to the full-size suppressor.

Figure 2 shows the design of a 20mm suppressor which was scaled from the results of the water table modeling tests. The pre-suppressor consists of a thick-wall cylinder (obtained by boring out a salvaged naval cannon) which contains thick-walled baffles separated by strong spacers. The second, larger, section is of somewhat lighter construction containing addition baffles separated again by spacers. Since the spacers and baffles are easily removed, the spacing thickness and number of baffles can be varied between firings if need be. Details and critical dimensions of the suppressor are summarized in a later section which describes the testing of the device.

A complete analytical description of the complicated series of events which occur within the suppressor during the barrel discharge is obviously not feasible. Even a casual observation of the water table simulation of the transient flow makes this fact abundantly clear. For that reason it was decided to break the analytical investigation of the fluid flow into two parts.

One part would be devoted to the analysis of the very strong initial shock wave whose propagation through the suppressor was observed on the water table to threaten the structural integrity of the suppressor. The predictions of this analysis would provide the designer with a feel

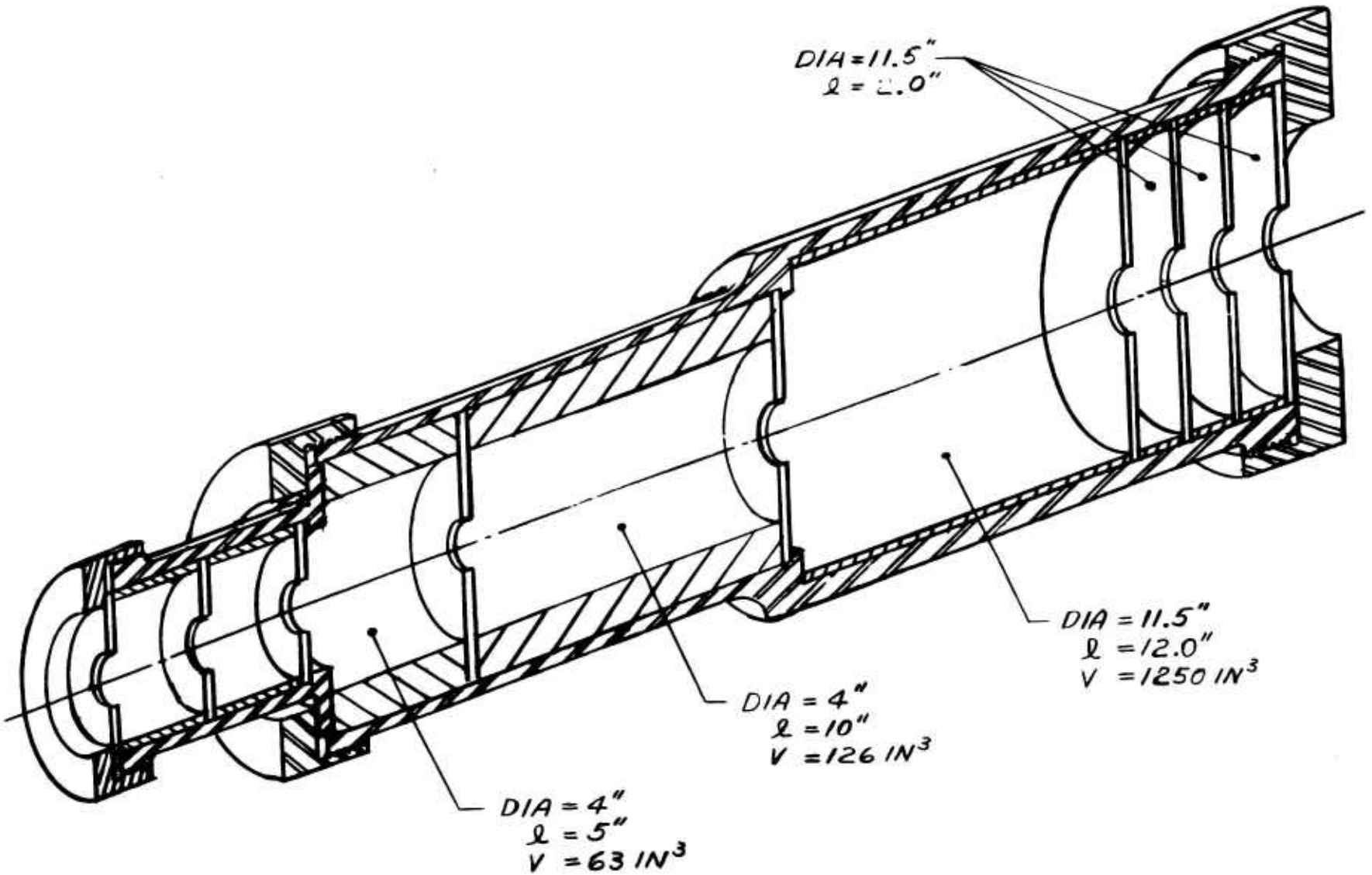

Figure 2. 20mm suppressor cutaway.

for the maximum impulsive pressures which might be imposed on various portions of the suppressor. The other part of the analysis would address itself to the unsteady bulk flow of barrel discharged gas through the suppressor following the establishment of the flow by the passage of the initial shock wave. The next section will address the first of these two analyses. A labelled line drawing of the suppressor is shown in Figure 3.

II.1. BLAST CHARACTERISTICS AT THE MUZZLE

The ballistic data for 20mm M3 cannons indicates that the muzzle uncorking pressure will be of the order 5000 psi and the projectile velocity about 2750 fps. The barrel gas temperature at uncorking is not given. It will therefore be estimated by assuming an isentropic compression

$$\frac{T_b}{T_o} = \left(\frac{P_b}{P_o}\right)^{\frac{\gamma_m - 1}{\gamma_m}} = \left(\frac{5000}{15}\right)^{1/5} = 3.2 \quad ; \gamma_m = 5/4$$

If the uncorking of the barrel is modeled as similar to the rupturing of a shock-tube diaphragm (Reference 2) the strength of the shock wave, P_{so}/P_o, created at the muzzle can be estimated from the equation

where

$$\frac{P_b}{P_o} = \frac{P_{so}/P_o}{\left\{1 - \left(\frac{P_{so}}{P_o} - 1\right)\left[\frac{\beta E}{\alpha_o \frac{P_{so}}{P_o} + 1}\right]^{1/2}\right\}^{1/\beta}}$$

$$\frac{c_{vo}}{c_{vm}} \approx 0.5 \; ; \; E = \frac{(cvT)_o}{(cvT)_m} = \frac{0.5}{32} = 0.1522 \; ; \; \beta = 0.1 \; ; \; \alpha_o = 9$$

---

[2] O.C. Bixler, "Analytical and Experimental Studies of Weapon Muffling", RIA 874, D.D.C., AD 821 879, Aug 1967

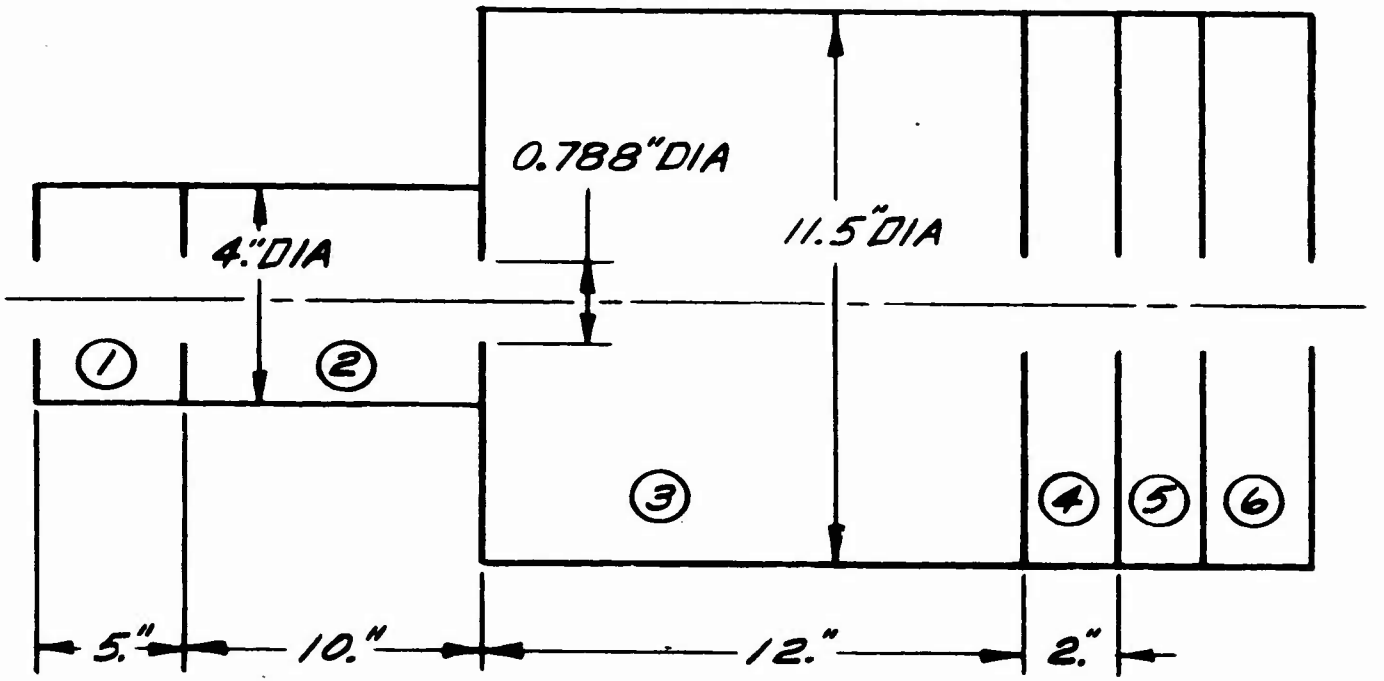

Figure 3. 20mm suppressor schematic.

With this data the implicit formula for the shock strength becomes

$$333 = \frac{P_{so}/P_o}{\left\{1-\left(\frac{P_{so}}{P_o}-1\right)\left[\frac{0.01562}{4P_{so}/P_o+1}\right]^{1/2}\right\}}$$

This equation is satisfied by the choice $P_{so}/P_o = 29$. The shock Mach number relative to the moving gas is then

$$M_{so} = \left[1+\left(\frac{P_{so}}{P_o}-1\right)\left(\frac{\gamma_o+1}{2\gamma_o}\right)\right]^{1/2} = 5.0 \quad ; \quad \gamma_o = 1.4$$

Since the propellant gas at the muzzle moves with the projectile's velocity the shock Mach number relative to a fixed reference frame (the ground) is

$$M_s = M_{so} + M_p = 5.0 + 2750/1100 = 7.5$$

II.2. BLAST CHARACTERISTICS IN THE FIRST CHAMBER

According to Reference 2 the shock wave in the first chamber has a Mach number given by the formula

$$M_1 = M\ {}'A_b/A_1)^{0.197}$$

where

A_b = area of a hemisphere having the diameter of the projectile

$$= \frac{\pi d^2}{2} = \frac{\pi}{2}(0.788)^2$$

A_1 = cross-sectional area of the expansion chamber

$$= \frac{\pi D^2}{4} = \frac{\pi}{4}(4)^2$$

Therefore

$$M_1 = 7.5\left[2\left(\frac{0.788}{4}\right)^2\right]^{0.197} = 4.53$$

---

[2] O.C. Bixler, "Analytical and Experimental Studies of Weapon Muffling", RIA 874, D.D.C., AD 821 879, Aug 1967

The pressure ratio across the shock wave incident upon the first baffle is

$$\frac{P_1}{P_0} = \frac{2\gamma_0}{\gamma_0+1}(M_1^2-1)+1 = 23.8$$

The pressure ratio across the shock wave reflected from the first baffle is given in Reference 3

$$\frac{P_{R1}}{P_1} = \frac{(1+2\mu^2)\frac{P_1}{P_0} - \mu^2}{1+\mu^2\left(\frac{P_1}{P_0}\right)}$$

where

$$\mu^2 = \frac{\gamma_0-1}{\gamma_0+1} = \frac{1}{6}$$

As a result $P_{R1}/P_1 = 6.53$ so that the first baffle must withstand a pressure difference

$$\Delta P_{R1} = \left(\frac{P_{R1}}{P_1}\frac{P_1}{P_0} - 1\right)15 = 2330 \text{ psi}$$

The water table experiments indicated that the side walls of the chamber would not be subjected to pressure differences as high as the baffle, but in the interest of safety it might be wise to design the whole chamber to withstand this pressure with an appropriate safety factor.

II.3. BLAST CHARACTERISTICS IN THE SECOND CHAMBER

The shock Mach number in the second chamber is given by the equation (Reference 2)

$$M_2 = M_1 \, (A_b/A_1)^{k_1/2}$$

---

[2] O.C. Bixler, "Analytical and Experimental Studies of Weapon Muffling", RIA 874, D.D.C., AD 821 879, Aug 1967

[3] D. Harleman, "Water Table Experiments on Transient Shock Wave Diffraction", Part I, AD 22 515, Aug 1953

where

A_b = area of hemisphere having the diameter of the baffle orifice

k_1 = 0.4, a function of M_1

If the baffle orifice diameter is 1.0"

$$M_2 = 4.53\ (1/8)^{0.2} = 2.99$$

The pressure ratio across the shock wave incident upon the second baffle is

$$P_2/P_o = 7/6\ (M_2^2 - 1) + 1 = 11.4$$

and the reflected pressure ratio is

$$P_{R2}/P_2 = 5.17$$

so that the pressure difference across the second baffle is

$$\Delta P_{R2} = \left(\frac{P_{R2}}{P_2} \frac{P_2}{P_o} - 1 \right) 15 = 885 \text{ psi}$$

II.4. BLAST CHARACTERISTICS IN THE THIRD CHAMBER

The area ratio across the second baffle is

$$A_o/A_3 = 2\ (d/D)^2 = 2\ (1/11.5)^2 = 1/66.2$$

The shock Mach number in the third chamber is

$$M_3 = M_2\ (A_o/A_3)^{0.41/2} = 1.27$$

while the pressure ratio across this shock is

$$P_3/P_o = 1.712$$

and the reflected pressure is

$$P_{R_3}/P_0 = 1.65$$

As a result, the third baffle will be subjected to a pressure differential

$$\Delta P_{R3} = 27.3 \text{ psi}$$

At this point, what was originally a very strong shock wave at the muzzle has degenerated to a strong acoustic - like wave. The theory used up to this point is valid only for strong shock waves and therefore cannot be used to evaluate the behavior of the remaining portion of the suppressor.

II.5. WAVE PROPAGATION THROUGH THE FINAL SERIES OF ORIFICES

The last series of orifices obviously function as a low-pass, almost linear, acoustic filters. The water table experiments revealed that the orifices in these baffles clip-off a portion of the incident shock wave which then radiates spherically from the down-stream side of the orifice into the next chamber. In this way each orifice acts as the source of a wave-front which is then spatially attenuated by the chamber between the baffles.

The spherical attenuation of the overpressure $\hat{p}(r)$ in the chamber following the orifice is given by the equation

$$\hat{p}(r) = \frac{R}{r}\,\hat{p}(R)$$

For the 20mm suppressor R = 1/2", r = 2" (baffle spacing distance) and $\hat{p}_3(R) = 0.712$ atm. from the previous calculations. At the fourth orifice $\hat{p}_4 = \frac{0.712}{4}$ atm. At the sixth orifice $\hat{p}_6 = \frac{0.712}{6}$ atm.

The sound pressure level of the shock wave emitted by the suppressor is computed from

$$SPL = 20 \log_{10}\left[\frac{\hat{p}_6}{2(10^{-10})}\right] = 154 \text{ db}$$

The sound pressure level of the shock wave at the gun muzzle is approximately 223 db. Since explosively generated shock waves are known to attenuate more severely with distance (near the source, i.e., r

< 50 ft.) than the acoustic wave, the predicted large reduction in source SPL will not be experienced in the far-field. Experience has shown (Reference 2) that maximum reductions of the order 30 in overall db levels are typical for the far-field. The foregoing calculations indicate that the proposed design might realize reductions of this magnitude.

It is known that at distances from the source greater than 50 feet the overall SPL of a small pressure wave attenuates more rapidly than the classical inverse radius relation predicts (Reference 4). This can be attributed to a number of factors related to meteorlogical conditions and terrain. It is also known that the higher frequency components of the signal are more severely attenuated by viscous dissipation than the low frequency components. Taken together, these vagaries make it extremely difficult to predict the expected shock wave db attenuation with distance as a function of the db reduction at the source.

II.6. ANALYSIS OF THE LOW FREQUENCY COMPONENTS OF THE SUPPRESSOR SIGNAL

As noted earlier the analysis of the flow through the suppressor is treated in two parts. Since it is known that the low frequency components are more weakly attenuated with distance from the suppressor or muzzle, the attenuation of these particular components by the suppressor is considered crucial to its successful operation. The lowest of these low frequency components fall in the range which can excite structural

---

[2] O.C. Bixler, "Analytical and Experimental Studies of Weapon Muffling", RIA 874, D.D.C., AD 821 879, Aug 1967

[4] G.R. Garinther, J.B. Moreland, "Acoustical Considerations for a Silent Weapon System - A Feasibility Study", Human Engineering Laboratory, AD 521 727 L, Oct 1966

vibrations in distant buildings and their contents. As a result they are considered to be most objectionable from a subjective point of view. The analysis presented in this section will be directed toward determining how effectively the proposed design attenuates this portion of the source signal's spectrum.

The sketch shown in Figure 3 shows the basic suppressor configuration. It has been simplified somewhat by omitting all but one of the last series of "acoustic" baffles. The general performance of the silencer is not drastically altered by this omission.

The low frequency components of the signal are associated with relatively long wave lengths. When these wave lengths are large with respect to the largest internal dimensions of the suppressor a lumped-parameter analysis may be employed. For the 20mm suppressor a lumped-parameter analysis would be expected to be applicable for frequencies less than 100 Hz which contains all the frequencies of interest.

If it is assumed that the pressure, density, etc. are essentially uniform throughout each chamber then the conservation of mass principle requires that for the first chamber

$$\dot{m}_o = V_1 \dot{\rho}_1 + \dot{m}_1$$

The pressure ratio across the first baffle will be quite large during most of the transient discharge process. That means that the orifice will be "choked" and the mass flow rate through it controlled only by the upstream gas thermodynamic coordiantes, i.e.,

$$\dot{m}_1 = K_1 \frac{P_1}{\sqrt{T_1}} = \mathcal{R} K_1 \sqrt{T_1}\, \rho_1$$

With this, the previous equation becomes

$$\dot{\rho}_1 + \frac{\mathcal{R} K_1 \sqrt{T_1}\, \rho_1}{V_1} = -\frac{V_b}{V_1} \dot{\rho}_b$$

$$\dot{\rho}_1 + \frac{\rho_1}{\tau_1} = -\frac{\dot{\rho}_b}{\tau_o}$$

In this equation τ_1 is the "time constant" for the first chamber, and γ_0 is the chamber to barrel volume ratio. The driving function $\dot{\rho}_b$ is a measure of how rapidly the barrel empties following its uncorking.

The conservation of mass equation for the second chamber takes the form

$$\dot{\rho}_2 + \frac{\mathcal{R} K_2 \sqrt{T_2}\, \rho_2}{V_2} = \frac{\mathcal{R} K_1 \sqrt{T_1}\, \rho_1}{V_1}$$

or

$$\dot{\rho}_2 + \frac{\rho_2}{\tau_2} = \frac{\rho_1}{\tau_{12}} .$$

For the third and last chamber

$$\dot{\rho}_3 + \frac{\mathcal{R} K_3 \sqrt{T_3}\, \rho_3}{V_3} = \frac{\mathcal{R} K_2 \sqrt{T_2}\, \rho_2}{V_3}$$

or

$$\dot{\rho}_3 + \frac{\rho_3}{\tau_3} = \frac{\rho_2}{\tau_{23}}$$

If it is assumed that the kinetic energy is completely recovered in each chamber (with small orifice to chamber diameter ratios and large orifice spacing it seems reasonable to assume little kinetic energy carry-over), then $\tau_1 \approx \tau_2 \approx \tau_3 \approx$ constant. The chamber "time constants" are given by the general relation

$$\tau = \frac{V}{K \sqrt{T}\, \mathcal{R}}$$

where

$$K = \left(\frac{2}{\gamma_m + 1} \right)^{\frac{\gamma_m + 1}{2(\gamma_m - 1)}} A_0 \sqrt{\frac{\gamma_m g_0}{\mathcal{R}}}$$

or

$$K \sqrt{T}\, \mathcal{R} = \left(\frac{2}{\gamma_m + 1} \right)^{\frac{\gamma_m + 1}{2(\gamma_m - 1)}} A_0 \sqrt{\gamma_m g_0 \mathcal{R} T}$$

(The quantity $\sqrt{\gamma_m g_o R T}$ = the characteristic sound speed of the gas.) Because the "time constants" are proportional to $(T)^{-1}/2$ they are not particular sensitive to modest changes in the absolute temperature. They will therefore be treated as constants, which for typical operating conditions are of the order

$$\tau = \frac{V}{A_o}(10^3) \quad sec^{-1}$$

It will be convenient to use the excess pressure $\hat{p}$ and the excess density $\hat{\rho}$ as dependent variables with the atmospheric density ρ_a as a reference level, i.e., $\rho_n = \rho_a + \hat{\rho}_n$. Substituting these into the previous relations gives

$$\dot{\hat{\rho}}_1 + \frac{\hat{\rho}_1}{\tau_1} = \frac{\hat{\rho}_b}{\tau_o}$$

$$\dot{\hat{\rho}}_2 + \frac{\hat{\rho}_2}{\tau_2} = \frac{\hat{\rho}_1}{\tau_{12}}$$

$$\dot{\hat{\rho}}_3 + \frac{\hat{\rho}_3}{\tau_3} = \frac{\hat{\rho}_2}{\tau_{23}}$$

where small order terms involving ρ_a have been neglected. The initial values of $\hat{\rho}_1$, $\hat{\rho}_2$ and $\hat{\rho}_3$ are zero.

Taking the Laplace transform of these equations and solving for the transform of $\hat{\rho}_3$ yields

$$\hat{\rho}_3(s) = \frac{-\frac{1}{\tau_{12}}\left(\frac{1}{\tau_{23}}\right)\frac{1}{\tau_o}\hat{\rho}_b(s)}{(s + 1/\tau_1)(s + 1/\tau_2)(s + 1/\tau_3)}$$

The exact nature of the density decay within the gun barrel is unfortunately not known. It will be assumed that a reasonable representation

is the function

$$\hat{\rho}_b = \hat{\rho}_m e^{-t/t_b}$$

so that

$$\dot{\hat{\rho}}_b = -\frac{\hat{\rho}_m}{t_b} e^{-t/t_b} = -\frac{\hat{\rho}_b}{t_b}$$

and

$$\hat{\rho}_3(s) = \frac{\tau_1 \tau_2 \tau_3}{\tau_{12} \tau_{23} \tau_0 t_b} \left[\frac{\hat{\rho}_b(s)}{(1+s\tau_1)(1+s\tau_2)(1+s\tau_3)} \right]$$

If the flow is essentially isothermal, then $\hat{\rho} \propto \hat{p}$. The spectral content of the excess pressure signal in the third chamber can therefore be determined by examining the Fourier transform of $\hat{\rho}_3(s)$ which is $\hat{\rho}_3(s=i\omega)$. The reduction in sound pressure level (SPL) at each frequency is given by

$$\Delta(SPL) = 20 \log_{10} \left\{ \frac{\tau_1 \tau_2 \tau_3}{\tau_{12} \tau_{23} \tau_0 t_b} \left| \frac{1}{(1+i\omega\tau_1)(1+i\omega\tau_2)(1+i\omega\tau_3)} \right| \right\}$$

III. MODEL EXPERIMENTS - 20MM SUPPRESSOR

III.1. ANALYSIS OF BLAST FIELD PRESSURE - TIME TRACES

Figures 4, 5, 6, and 7 show the model suppressor and its installation at the Malta Test Station. Figures 8-11 illustrate typical pressure-time traces from a transducer located according to the plan-view sketch of Figure 12.

The first two spikes on the pressure recording can be attributed to the passage of the projectiles direct pressure wave followed by its ground reflection. This suspicion is fortified by comparing Figures 8 and 9 which are generally similar in shape except for the absence of these two spikes in Figure 9 when no projectile was actually fired. A simple analysis of the projectile's shock wave propagation shows that the time delay between the initial shock wave's arrival at the transducer and its ground reflection's arrival is given by

$$\delta t = \frac{\cos \alpha}{v_s} \left[|r_2 - r_1| + r_3 \right]$$

where

$$\sin \alpha = \frac{1}{M_p} = \frac{v_s}{v_p}$$

Figure 13 shows the distances r_1, r_2, and r_3 which are measured in a vertical plane normal to the flight path containing the pressure transducer.

Figure 4. View of 20mm gun showing transducer.

Figure 5. View of 20mm gun with suppressor.

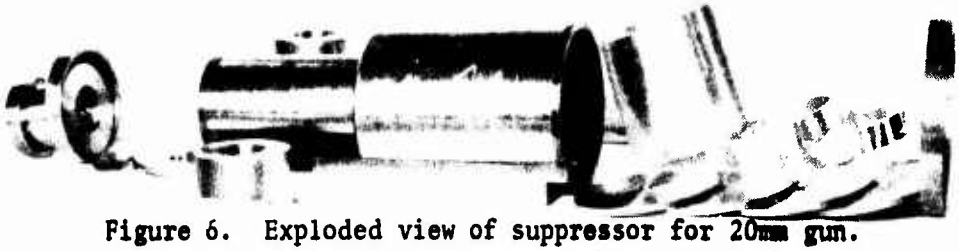

Figure 6. Exploded view of suppressor for 20mm gun.

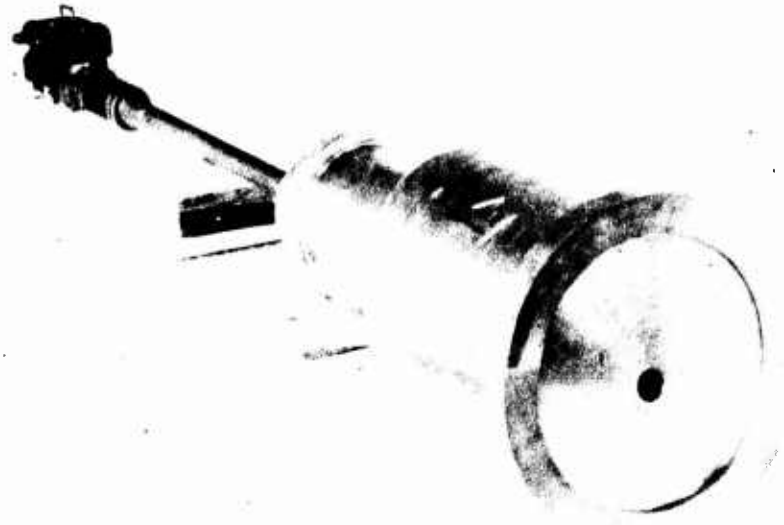

Figure 7. Close-up of suppressor.

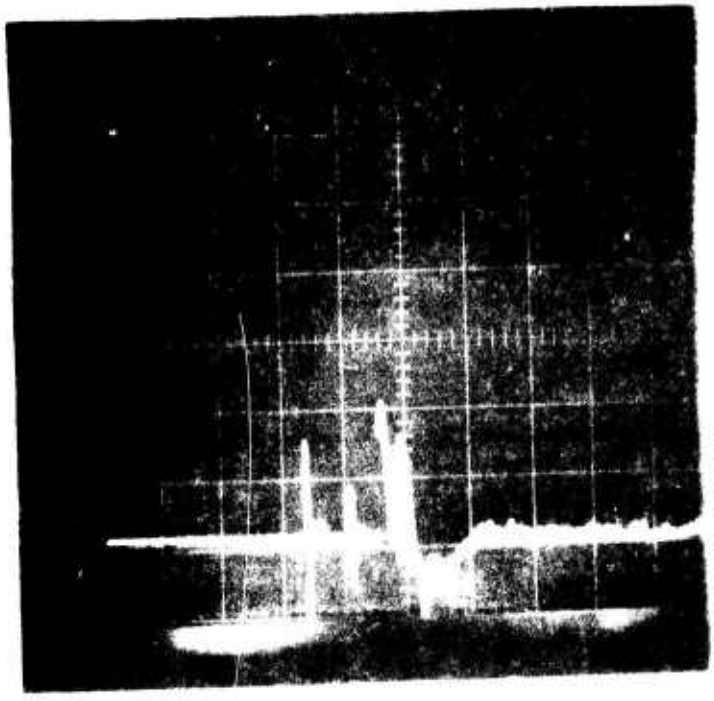

FIGURE 8

ROUND NO. 8-NS

SENSITIVITY:
.2 PSI/DIV.

SWEEP SPEED:
5 M.S./DIV.

SENSOR DISTANCE
ABOVE GROUND:
4 FT.

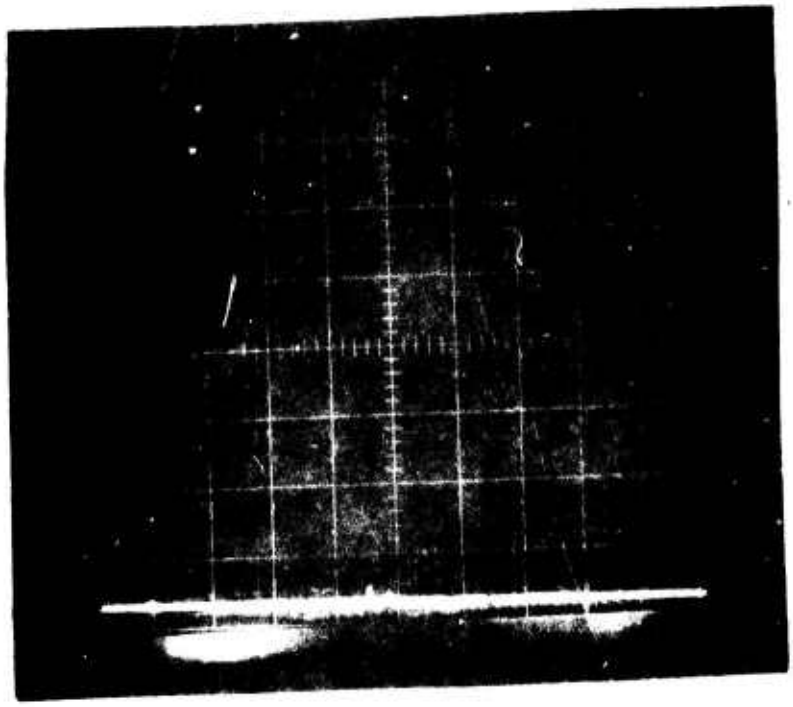

FIGURE 9

ROUND NO. 9*

SENSITIVITY:
.2 PSI/DIV.

SWEEP SPEED:
5 M.S./DIV.

SENSOR DISTANCE
ABOVE GROUND:
4 FT.

* PRIMER ONLY
(NO POWDER OR
PROJ.)

When the transducer is 4 feet off the ground , (Figures 8, 11) the measured delay time is about 3.8 milliseconds. The projectile Mach number is thought to be approximately 2.5. Assuming that the shock wave travels at a speed of approximately 1100 fps (conservatively) the computed delay time is 4.7 ms. For pressure transducer located 7 feet off the ground (Figure 10) the computed delay time is 5.9 ms. A comparison of Figures 8 and 10 shows that the ground reflected spike appears in Figure 10 in the midst of the muzzle blast signal, about 7 ms following the initial spike. The traces shown in Figures 8 and 11 represent "cleaner" signals than that of Figure 10 since these traces, obtained from the lower transducers, separate the projectile signal from muzzle blast signal.

Reference 4 gives the following formula for the time duration of the projectile's N-shaped shock wave

$$T = \frac{1.82\, M_p\, d_p}{c\,(M_p^2 - 1)^{3/8}} \left(\frac{y}{L}\right)^{1/4}$$

At a transducer distance of y = 4 feet, for a 20mm projectile

$$T = \frac{1.82\,(2.5)\,0.768}{1100\,(5.25)^{3/8}\,12} \left(\frac{4}{1/4}\right)^{1/4} = 0.293 \text{ ms}$$

The shock duration is only slightly longer for $y = r_1 = 8.05$ ft corresponding to the 7 foot transducer elevation. These predictions are certainly comparable to the short spike durations indicated in the pressure-time traces.

This same reference gives the projectile's shock wave overpressure as

$$\frac{\hat{P}_p}{P_o} = \frac{0.53\,(M_p^2 - 1)^{1/8}}{y^{3/4}} \left(\frac{d_p}{L^{1/4}}\right)$$

[4] G.R. Garinther, J.B. Moreland, "Acoustical Considerations for a Silent Weapon System - A Feasibility Study", Human Engineering Laboratory, AD 521 727 L, Oct 1966

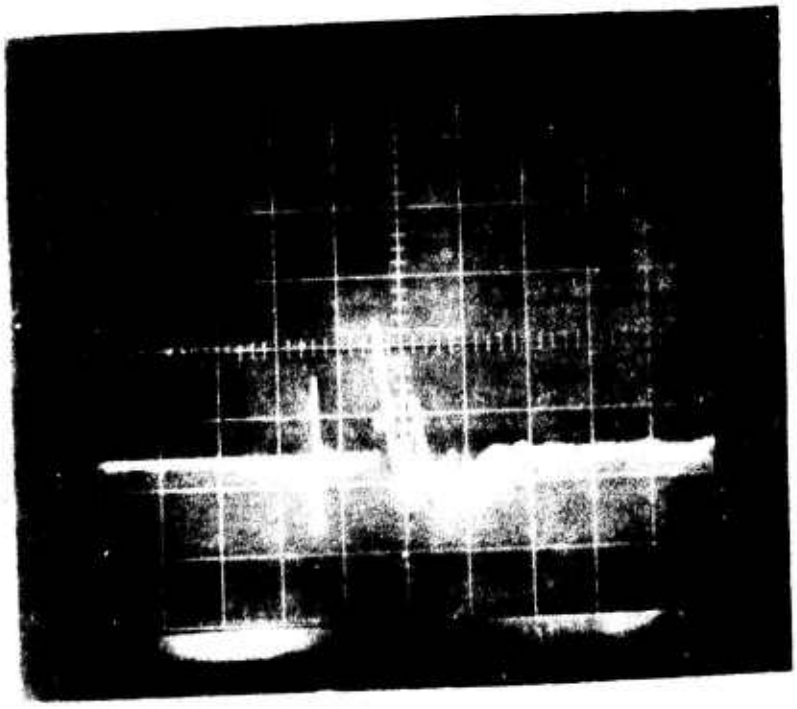

FIGURE 10

/ROUND NO. 10-NS

SENSITIVITY:
.2 PSI/DIV.

SWEEP SPEED:
5 M.S./DIV.

SENSOR DISTANCE
ABOVE GROUND:
7 FT.

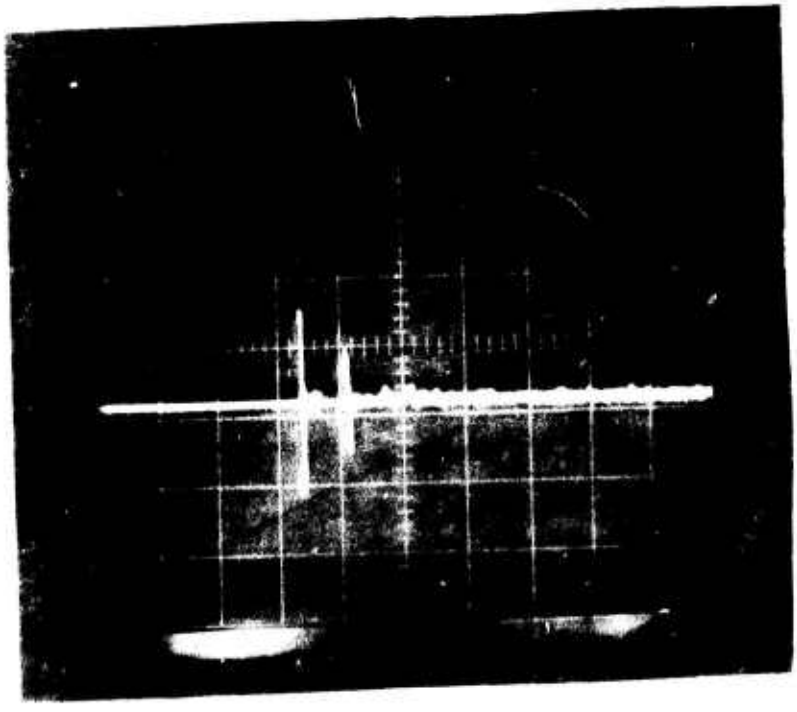

FIGURE 11

ROUND NO. 13-S

SENSITIVITY:
.2 PSI/DIV.

SWEEP SPEED:
5 M.S./DIV.

SENSOR DISTANCE
ABOVE GROUND:
4 FT.

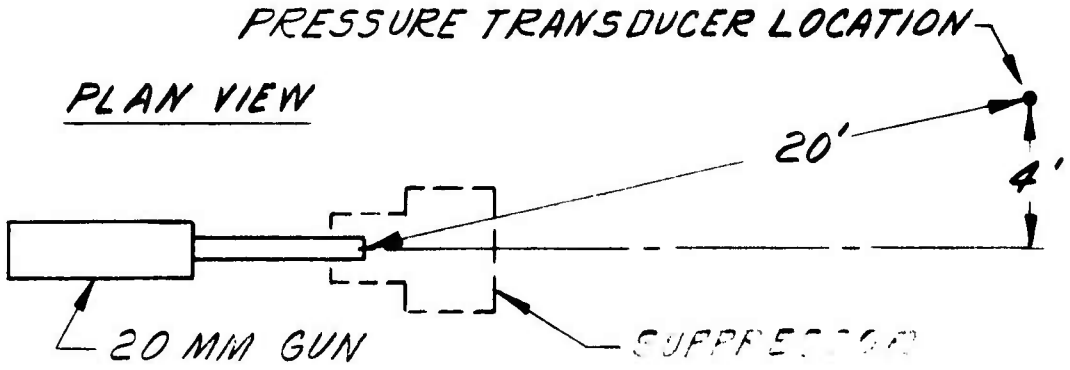

Figure 12. Transducer location, 20mm tests.

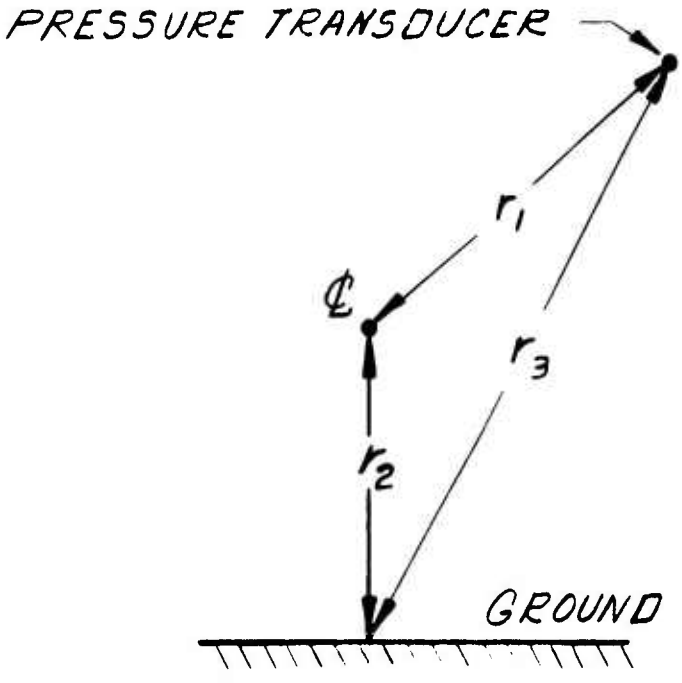

Figure 13. View along projectile light path.

For the lower transducer position the equation predicts $\hat{P}_p = 0.3$ psi and for the higher position $\hat{P}_p = 0.2$ psi . The measured values are 0.14 and 0.12 psi respectively, roughly about one-half the predicted values. A crude calculation of the attenuation of the muzzle blast wave indicates the same discrepancy. Taking $P_{30}/P_0 = 29$, the barrel diameter = 0.8", and the distance to the transducer = 20 feet, and assuming that the shock wave decays according to the inverse distance law, yields a muzzle blast shock wave pressure at the transducer of

$$\hat{P}_{shock} = \frac{P_{30}}{P_0}\left(\frac{r}{R}\right)P_0 = 29\left(\frac{0.8}{20(24)}\right)15.0 = 0.71 \text{ psi}$$

This is roughly twice the measured maximum of the muzzle blast signal.

The projectile shock wave Mach number can be calculated from the familiar formula

$$M_s = \left[\frac{\gamma_0+1}{2\gamma_0}\left(\frac{P_3}{P_0}\right) + \frac{\gamma_0-1}{2\gamma_0}\right]^{1/2}$$

Using the previously computed overpressure , M_s is predicted to be 1.01 as assumed in earlier calculations.

There are several conclusions which can be drawn from the foregoing analysis. The first is that the ground reflected signal is quite strong and, depending on the location of the transducer, it can distort the direct signals received by the transducer. The second tentative conclusion is that the pressure transducer seems to read peak pressures which are conservative (about 1/2 the expected value), possibly due to the response characteristics of the the instrumentation itself.

The latter portion of the signal trace caused by the muzzle blast would be expected to look like the typical time decaying N-wave produced by most weapon discharges. Figure 11 shows that this latter portion of the trace is greatly attenuated by the suppressor as expected,

while the spikes attributed to the projectile shock wave persist. Figure 8 has the typical blast signal shape but with two positive initial pressure peak instead of one. Figure 10 has the same two peaks with the reflected projectile spike sandwiched between them. In both figures the second of the two large positive pressure peaks are clearly caused by the ground reflection of the muzzle blast wave.

Unfortunately this reflected signal arrives at the transducer in time to intermingle with the direct blast wave so that the recorded signal is actually a superposition of the two signals (along with the reflected projectile signal in Figure 10). Despite the fact that this latter portion of the trace is "dirty" it is still possible to draw some conclusions from it. Obviously the first peak represents the measured maximum pressure rise of the blast. The minimum negative value recorded is probably a superposed value which may or may not be indicative of the actual minimum depending on the time delay between the direct and reflected signals. The overall duration of the actual signal is somewhat less than the recorded value due to this time delay.

Contrary to the projectile induced shock wave which forms a conical envelope, the muzzle blast propagates roughly as a spherical front centered at the muzzle or suppressor outlet. Figure 14 shows the geometry for the direct blast wave and the reflected wave represented by the image muzzle. The time delay between the direct signal and the reflected signal is given by

$$\Delta t = \frac{r_2 - r_1}{v_0}$$

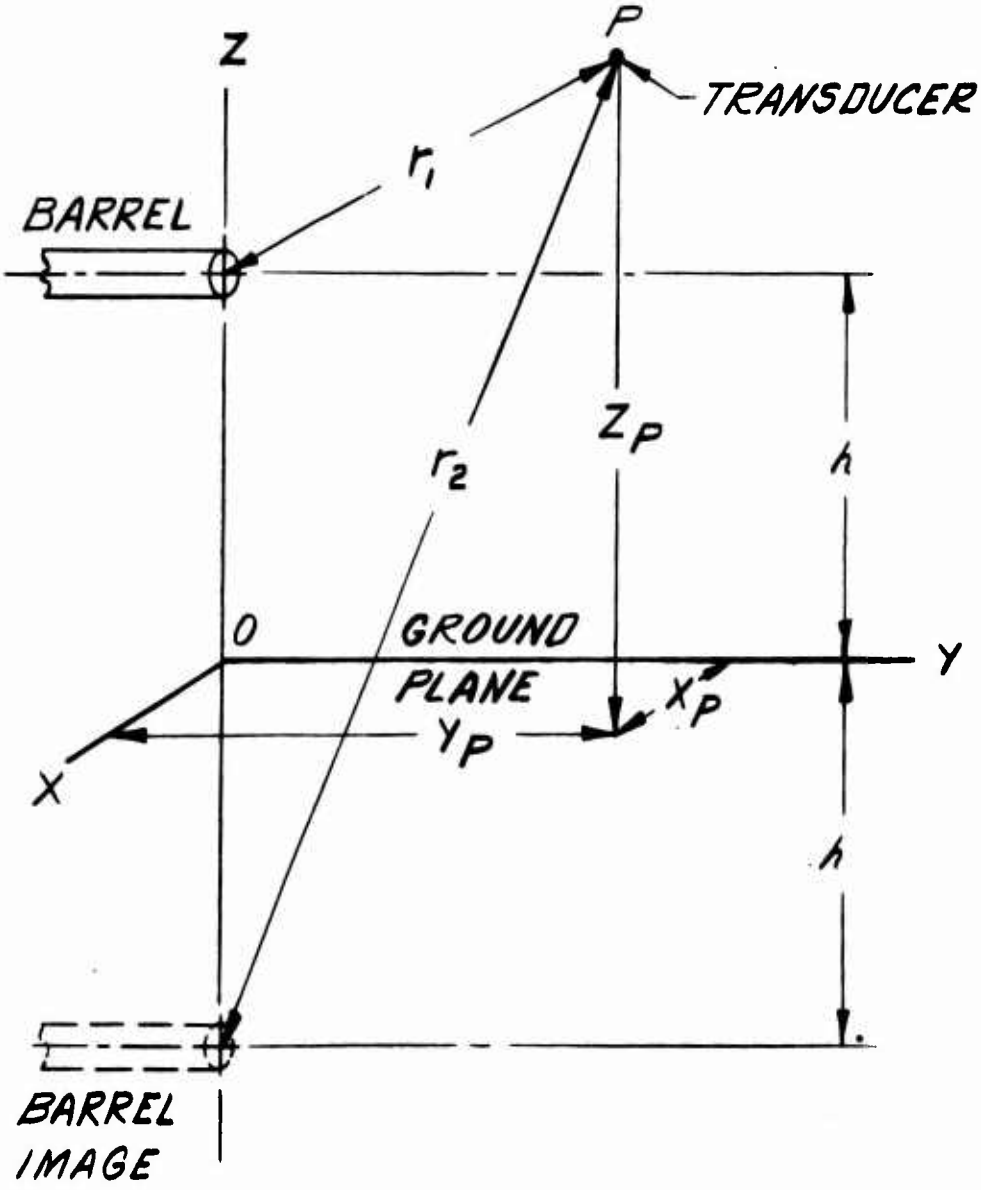

Figure 14. Muzzle blast shock wave geometry.

where

$$r_1^2 = x_p^2 + y_p^2 - (z_p - h)^2$$

$$r_2^2 = x_p^2 + y_p^2 + (z_p + h)^2$$

and v_b = blast wave propagation velocity

Assuming that v_b = 1100 ft/sec the delay time between the two positive pressure peaks are computed to be 1.47 ms and 2.46 ms for the 4 feet and 7 feet high transducer positions. The measured delay times are 1.6 ms and 3.0 ms respectively. Thus the first portion of the blast signal (i.e., the abrupt rise and rapid decay to negative values) is a record of the direct blast, and the rest of the record is a mixture of direct and reflected waves.

If it is assumed that the blast wave overpressure follows the classical relation

$$\hat{p} = \hat{p}_{max} \left(1 - \frac{t}{t_o}\right) e^{-t/t_o}$$

then

$$\hat{p} = 0 \quad \text{at} \quad t/t_o = 1$$

$$\hat{p} = \hat{p}_{min} \quad \text{at} \quad t/t_o = 2$$

and

$$\left| \frac{\hat{p}_{max}}{\hat{p}_{min}} \right| = e^2 = 7.4$$

The two to one time scale given in the first set of relations cannot be verified for the direct signal due to the masking effect of the reflections. If the second peak and recorded minimum are selected a two to one time scale is actually measured.

The theoretical amplitude ratio is much larger than any of the measured ratios which are of the order 2 to 3. This discrepancy is probably due in part to the cancelling effect of the superposed signals and indequacies in the instrumentation.

To summarize, the salient features of Figures 8, 9, and 10 can be interpreted logically based on a straight-forward analysis of the projectile and muzzle blast generated pressure signals. The recorded time scales of the various events are reasonably close to those predicted from simple geometric considerations. The amplitudes of the recorded signals, however, are consistantly lower than those expected by at least a factor of two or more. Most important of course is the comparison between Figure 11 and Figures 8 and 10 which indicate the relative effectiveness of the device as a suppressor of the muzzle blast pressure signal. This comparison clearly illustrates the degree to which the suppressor attenuates the noise generated by the muzzle blast.

III.2. ANALYSIS OF SPECTRAL CONTENT OF THE 20MM SIGNAL AT 100 METERS

Figure 15 shows the spectral content of the signal received at 100 meters to the side and slightly behind the 20mm gun. This plot results from the 1/3 octave band spectral analysis of an F. M. tape recording of the overpressure made on site by Mr. D. Driscoll of the N. Y. S. Environmental Conservation Department.

If it is assumed that the muzzle blast signal is described by the classical equation

$$\hat{\rho} = \hat{\rho}_{max} \left(1 - \frac{t}{t_o}\right) e^{-t/t_o}$$

the Fourier transform of the blast signal is then given by

$$\left| \frac{\tilde{F}(\omega)}{\hat{\rho}_{max}\, t_o} \right| = \left| \frac{\omega t_o}{1 + (\omega t_o)^2} \right|$$

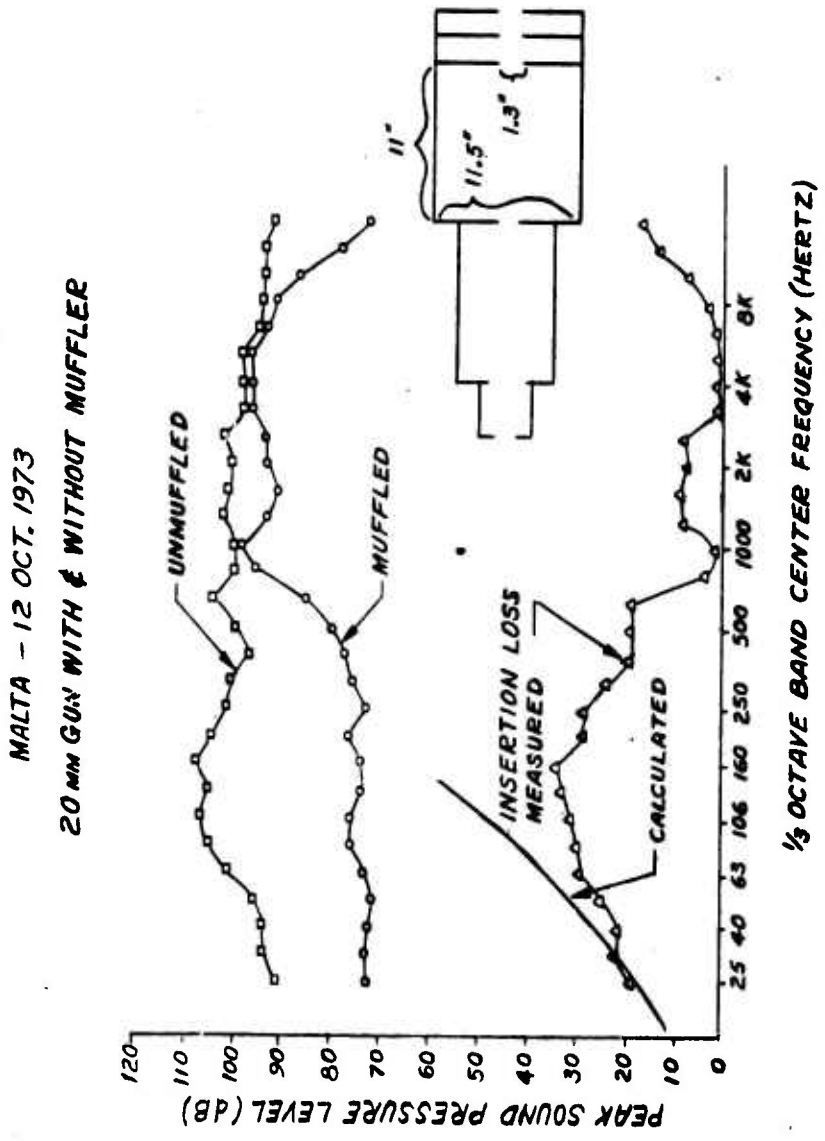

Figure 15. Frequency spectrum, 20mm gun.

The value of t_0 is estimated from Figures 8 and 10 to be about 1.2 ms. The following table illustrates the distribution of the muzzle blast relative amplitude with frequency.

f	$\frac{\omega t_0}{1+(\omega t_0)^2}$
25	0.180
50	0.331
100	0.480
500	0.248
1,000	0.130
4,000	0.033

The peak relative amplitude occurs when $wt_0 = 1.0$ which corresponds to f = 132 Hz.

If it is assumed that the shock wave caused by the projectile is the typical "N" wave* then the Fourier transform of that signal is given by

$$\left| \frac{F(\omega)}{\hat{p}_p \tau} \right| = 2 \left| \frac{\omega\tau \cos\omega\tau - \sin\omega\tau}{(\omega\tau)^2} \right|$$

where $\tau = \frac{T}{2} \approx 0.15$ ms from the previously calculated results. A tabulation of the relative amplitude as a function of frequency is given in the following table:

f	$\frac{\omega\tau\cos\omega\tau - \sin\omega\tau}{(\omega\tau)^2}$
25	negligible
50	negligible
500	0.149
1,000	0.285
4,000	0.174
10,000	0.106

Inspection of Figure 15 shows that the unmuffled signal is quite flat over the range 25 to 8,000 Hz with a faint peak at about 120 Hz.

*The position of the microphone 100m to the side and slightly behind the muzzle makes this a somewhat tenuous assumption.

Comparing this with the computed amplitude-frequency results indicates that the recorded signal is apparently composed of a muzzle blast signal centered at about 120 Hz superposed on the somewhat weaker projectile shock wave centered at about 1,000 Hz. This same relative magnitude of the two signals is also indicated in Figures 8 and 10. The total unmuffled signal is probably a weak bi-modal distribution in which the two contributing modes overlap somewhat in the range 500 to 1,000 Hz.

The suppressor is intended to filter out a portion of the muzzle blast, but obviously can have no effect whatsoever on the projectile blast. Inspection of the muffled data plotted on Figure 15 supports the contention that original signal is composed of two signals, since a substantial reduction of signal amplitude is noted in the range 25 to 500 Hz, but little effect is found at the higher frequencies. If this is the correct interpretation of the results shown in Figure 15, one must conclude that the suppressor reduced the muzzle blast amplitudes by roughly 30 db in the range 25 to 500 Hz. This is the same order of magnitude reduction which has been obtained using a similarly designed suppressor to silence small arms (Ref. 2) and probably represents the upper limit of suppression which is feasible. Since it is known that the higher frequency components of a signal tend to decay more rapidly with distance than the low frequency components the inability of this device to attenuate this projectile generated frequencies should not represent a serious noise problem at large distances from the muzzle when small projectiles are used.

[2]O.C. Bixler, "Analytical and Experimental Studies of Weapon Muffling", RIA 874, D.D.C., AD 821 879, Aug 1967

In a previous section it was estimated that the reduction in sound pressure level was given by the expression

$$\Delta(SPL) = 20\log_{10}\left(\frac{\tau_1\,\tau_2\,\tau_3}{\tau_{12}\,\tau_{23}\,\tau_0\,t_b}\right) + 20\log_{10}\left|\frac{1}{(1+i\omega\tau_1)(1+i\omega\tau_2)(1+i\omega\tau_3)}\right|$$

The approximate calculated value of $\frac{\tau_1\,\tau_2\,\tau_3}{\tau_{12}\,\tau_{23}\,\tau_0\,t_b}$ is 0.6 $(t_b \sim 6\ ms)$. The following table shows the computed values of the second term in the expression for Δ (SPL)

f (Hz)	$20\log_{10}\left\|\frac{1}{(1+i\omega\tau_1)(1+i\omega\tau_2)(1+i\omega\tau_3)}\right\|$
1.59	-0.15
5.03	-1.475
15.9	-9.45
25.0	-15.9
47.7	-30.0
100	-48.0
150	-58.5

Since the lumped-parameter analysis is approximate it is expected that it will represent qualitiative trends in performance more accurately than quantitative ones. In a practical sense one would not expect the suppressor amplify a D.C. signal $(t_b \to \infty, \omega \to 0)$ i.e., increase the discharge pressure or density relative to the source pressure or density when the input signals are steady.

Two calculated results are plotted in Figure 15. One curve was obtained assuming that $\log_{10}\left|\frac{\tau_1\,\tau_2\,\tau_3}{\tau_{12}\,\tau_{23}\,\tau_0\,t_b}\right| = 0$ and the other using $20\log_{10}(0.6) = -4.45$ db . The first curve results from the arbitrary assumption that the approximations in the analysis can be empirically compensated for by taking $\frac{\tau_1\,\tau_2\,\tau_3}{\tau_{12}\,\tau_{23}\,\tau_0\,t_b} = 1.0$ rather than 0.6 as estimated.

The second curve yields somewhat larger attenuations due to the D.C. contribution. In either case it is observed that the predictions with regard to trend and magnitude are reasonably correct for $25 Hz < f < 100 Hz$. The 100 Hz limit was previously estimated to be a delimiting value for the analytical model.

The analysis of the frequency content of the suppressed and unsuppressed pressure signals can be summarized as follows:

1. The spectral content of the unsuppressed signal is composed of two components of nearly equal maximum amplitude. One predominantly low frequency mode is associated with the muzzle blast and the other predominantly higher frequency mode is associated with the projectile shock wave.

2. The center frequency separation and band widths of each of the contributing modes are such that the combined bi-modal unsuppressed signal is quite flat in the range $100 < f < 10{,}000$ Hz.

3. The suppressor, which acts as a low-pass filter for the muzzle blast, quite effectively reduces that portion of the signal contributed by the muzzle blast, but, as expected, does nothing to reduce the projectile's contribution.

4. The-lumped parameter analysis of the low frequency attenuating characteristics of the suppressor compares reasonably well with the measured attenuation in the frequency range for which the analysis is expected to be valid.

5. The simple analytical techniques derived from theoretical considerations appear to be an adequate basis for modeling the 20mm results to full-scale prototype design.

IV. PREDICTED PERFORMANCE CHARACTERISTICS OF A 155MM GUN BLAST SUPPRESSOR

The most severe firing conditions for a 155mm gun are assumed to be $P_0 = 9000$ psi (uncorking pressure) and a 1,850 ft/sec projectile velocity. The barrel gas uncorking temperature is estimated to be

$$\frac{\bar{T}_b}{T_0} = \left(\frac{9000}{15}\right)^{1/5} = 3.6$$

and

$$E = \frac{(c_v T)_0}{(c_v T)_m} = \frac{0.5}{3.6} = \frac{1}{7.2}$$

The pressure ratio $\frac{P_{30}}{P_0}$ across the shock generated by the uncorking process is given by

$$600 = \frac{P_{30}/P_0}{\left\{1-\left(\frac{P_{30}}{P_0}-1\right)\left[\frac{0.0139}{1+9\,P_{30}/P_0}\right]^{1/2}\right\}^{10}}$$

Assuming $P_{30}/P_0 = 39$, the right hand side of this equation becomes

$$\frac{39}{\left\{1-38\left[\frac{0.0139}{352}\right]^{1/2}\right\}^{10}} = \frac{39}{\left\{1-\frac{38}{159}\right\}^{10}} = 600$$

The shock Mach number is then

$$M_{30} = \left[1+\left(\frac{P_{30}}{P_0}-1\right)\frac{\gamma_0+1}{2\gamma_0}\right]^{1/2}; \quad \gamma_0 = 1.4$$

The propellant gas Mach number is

$$M_3 = M_{30} + M_p = 5.8 + \frac{1850}{1100} = 7.48$$

Figure 16 shows the proposed suppressor design. The shock wave in the first chamber has a Mach number

$$M_1 = M_3\left(\frac{A_b}{A_1}\right)^{0.197}$$

where

$$A_b = 2\left(\frac{\pi d^2}{4}\right) = \frac{\pi}{2}(6.1)^2$$

so that

$$A_1 = \frac{\pi D^2}{4} = \frac{\pi}{4}(24)^2$$

$$\frac{A_b}{A_1} = 2\left(\frac{6.1}{24}\right)^2 = \frac{1}{7.72}$$

and

$$M_1 = 7.48\left(\frac{1}{7.72}\right)^{0.197} = 5.0$$

The pressure ratio across the incident shock wave is

$$\frac{P_1}{P_0} = \frac{7}{6}(M_1^2 - 1) + 1 = \frac{7}{6}(24) + 1 = 29$$

The pressure ratio across the reflected shock wave is

$$\frac{P_{R1}}{P_1} = \frac{(1 + 2\mu^2)\,P_1/P_0 - \mu^2}{1 + \mu^2\,P_1/P_0}$$

where

$$\mu^2 = \frac{\gamma_0 - 1}{\gamma_0 + 1} = \frac{1}{6}$$

Therefore

$$\frac{P_{R1}}{P_1} = \frac{8(29) - 1}{6 + 29} = 6.35$$

so that the first baffle must withstand a pressure of

$$\Delta\hat{P}_{R1} = \left(\frac{P_{R1}}{P_1}\frac{P_1}{P_0} - 1\right)P_0 = \left[6.35(29) - 1\right]15 = 2750\,psi$$

The water table results for a two-dimensional scaled simulation yielded estimated pressures in the range 2,400 to 3,800 psi for a barrel pressure of 15,000 psi.

The shock Mach number in the second chamber is given by

$$M_2 = M_1\left(\frac{A_0}{A_1}\right)^{R_1/2}$$

which becomes

$$M_2 = 5.0\left(\frac{1}{7.72}\right)^{0.2} = 3.32$$

The pressure ratio across this shock wave is

$$P_2/P_0 = \frac{7}{6}(M_2^2 - 1) + 1 = 12.65$$

The pressure ratio across the shock wave reflected from the second baffle is

$$\frac{P_{R2}}{P_2} = \frac{8(12.65) - 1}{6 + 12.65} = 5.36$$

The second baffle must therefore withstand a pressure of

$$\Delta\hat{P}_{R2} = \left(\frac{P_{R2}}{P_2}\frac{P_2}{P_0} - 1\right)P_0 = \left[5.36(12.65) - 1\right]15 = 1000\,psi$$

The water table test results yielded baffle pressures in the range 1,000-1,400 psi.

The area ratio is

$$\frac{A_0}{A_3} = 2\left(\frac{d}{D}\right)^2 = 2\left(\frac{6.1}{86}\right) = \frac{1}{99.5}$$

so that the Mach number is

$$M_3 = M_2\left(\frac{A_0}{A_3}\right)^{K_2/2} = 3.32\left(\frac{1}{99.5}\right)^{0.205} = 1.29$$

The pressure ratio across this shock is

$$P_3/P_0 = \frac{7}{6}(M_3^2 - 1) + 1 = \frac{7}{6}(0.665) + 1 = 1.776$$

The pressure ratio across the reflected shock wave is

$$P_{R3}/P_3 = \frac{8(1.776) - 1}{6 + 1.776} = 1.70$$

The third baffle must withstand a pressure of

$$\Delta\hat{P}_{R3} = \left(\frac{P_{R3}}{P_3}\frac{P_3}{P_0} - 1\right)P_0 = \left[1.7(1.776) - 1\right]15 = 30.3\,psi$$

The water table experiments yielded pressures on this baffle of 140 to 180 psi. Malta measured about 100 psi in their unbaffled cylinder.

The propagation of the nearly acoustic wave overpressure through the last four baffles is given by

$$\hat{p}(r) = \frac{R}{r}\hat{p}(R) = \frac{3}{24}(0.776) \approx 0.1\ bars$$

At the silencer exit orifice

$$\hat{p}_6 = \frac{0.1}{64} \approx 2(10^{-2})\ bars$$

The sound pressure level of the shock wave emitted by the suppressor is computed to be

$$SPL = 20\log_{10}\left[\frac{2(10^{-2})}{2(10^{-10})}\right] = 160\ dB$$

which is roughly comparable to that emitted by the 20mm suppressor. Presumably the peak pressures measured by transducers (located in the same relative positions as those used in the 20mm tests) would indicate roughly the same overpressures as recorded in the model tests.

The time constant, t_0, of this blast wave would be expected to be somewhat longer than the recorded 1.3 ms for the 20mm. This would shift the peak amplitude to a frequency below 100 Hz. The full scale suppressor shown in Figure 16 has the following time constants:

$$\tau_1 = 32(10^{-3})\ sec$$

$$\tau_2 = 64(10^{-3})\ sec$$

$$\tau_3 = 4100(10^{-3})\ sec$$

The lumped-parameter analysis for a suppressor of this size would be expected to be valid up to frequencies of approximately f = 5 Hz. The following table shows the predicted relative attenuation of the proposed 155mm suppressor at these low frequencies

f (Hz)	$20\log_{10}\left\lvert\frac{1}{(1+i\omega\tau_1)(1+i\omega\tau_2)(1+i\omega\tau_3)}\right\rvert$
1.59	-34.2
5.03	-50.5

If it is assumed that t_0~10 ms for a 155mm the peak amplitude in the muzzle blast spectrum would occur at $\omega t_0 = 2\pi f t_0 = 1.0$

$$f = \frac{1}{2\pi t_0} = \frac{100}{2\pi} = 15.9\ Hz$$

which is well above the low-pass range of the suppressor.

For a projectile 24" long, 6.1" diameter traveling at $M_p = 1.68$, the shock wave generated peak overpressure is (for the lower transducer)

$$\frac{\hat{P}_p}{P_o} = \frac{0.53(M_p^2-1)^{1/8}}{y^{3/4}}\left(\frac{d}{L^{1/4}}\right) = \frac{0.53\,(1.078)\,6.1}{(48)^{3/4}(24)^{1/4}} = 8.62\,(10^{-2})$$

or $\hat{P}_p = 1.27$ psi. At the higher transducer the overpressure would be 0.846 psi.

The time duration of the projectiles N-wave is given by

$$T = \frac{1.82\,M_p\,d}{c(M_p^2-1)^{3/8}}\left(\frac{y}{L}\right)^{1/4} = \frac{1.82\,(1.68)\,6.1}{1100[(1.68)^2-1]^{3/8}\,12}\left(\frac{4}{2}\right)^{1/4} = 1.35(10^{-3})\text{ sec}$$

As expected the "ballistic crack" produced by the projectile will be somewhat more intense than that caused by the 20mm gun. The duration of this noise will be longer and contain lower frequency components so that the peak amplitude will occur at about 200 Hz. The combination of larger overpressures concentrated at lower frequencies means that the "ballistic crack" produced by a 155mm projectile will remain audible at greater distances than the 20mm. The higher frequency components of this signal will be progressively filtered-out with increasing distance from the source by viscous dissipation. At large distances the original "crack" will be reduced to a rumble similar to, but not as intense as, a sonic boom. Whether or not this sound will remain objectionable to the listener remains an open question.

To summarize:

1. The 155mm proposed design will effectively filter out frequency components of the muzzle blast above 1 Hz.

2. The center frequency of the muzzle blast is estimated to be 15 Hz.

3. The maximum projectile ballistic crack amplitude is expected to occur at about 200 Hz. As expected the amplitude and duration of this signal will be considerably larger than for a 20mm projectile.

4. Because the projectile noise is concentrated at lower frequencies then will be less viscous attenuation of the projectile noise than with the 20mm.

5. The suppressor will probably remove approximately 20-30 db from the muzzle blast signal while leaving the projectile signal untouched.

6. The projectile signal may be audible at considerable stand-off distances, and may still be judged objectionable by the listener.

V. TESTS OF A SIMPLIFIED FULL SCALE DESIGN

Although every reasonable precaution has been taken up to this point in the program to ensure that final design decisions were based on the best information available, several elements of failure-risk still existed. These uncertainties fell into two general categories:

1. Structural integrity
2. Sound reduction

The first of these had not been investigated since the only field tested suppressor was the 20mm model which was structurally overdesigned for safety reasons. The answer to the second question was uncertain because the modeling laws for scaling (i.e. dimensionless numbers) had not yet been established. True, the analysis of the 20mm model and its performance had been rationalized but since a general theory for suppressor performance was not proven or even known, there was no quarantee

that the full-scale design would perform acoustically as designed. Although the latter is a subtle point and one which is often ignored in the press of time and funds, it is a very real one. To put it simply, when approximate analyses are proposed their predictions should be verified by testing more than one size device . This had not yet been done at this stage of the program.

Considering the cost of constructing a full-scale suppressor based on the paper design and the uncertainties which still existed concerning its performance, it was decided instead to fabricate an inexpensive, albeit crude, replica of the full-scale device. In order to keep costs within bounds, it was found necessary to sacrifice certain physical modeling details while at the same time retaining the essential, broad features of the proposed design. Figure 17 illustrates this compromised design. At the left end, the first chamber consists of an extremely strong, cylindrical vessel originally used as a "wrapper" or container in which turbine wheels were burst in overspeed tests. The walls of the wrapper were 2" thick and the end plates were 3" thick. The end plates were bolted to the cylindrical side of the wrapper and had 20" diameter holes centrally located in them. Although somewhat larger in volume than called for in the paper design, this salvaged vessel served as an almost ideal first, high pressure chamber of the high-low design. To the right of the wrapper in the direction of projectile flight, are two railroad tank car tanks whose end plates have been removed. These cylinders had a wall thickness of 1/2". Two cylinders were tied together by welded-on straps and cables which prevented the relative

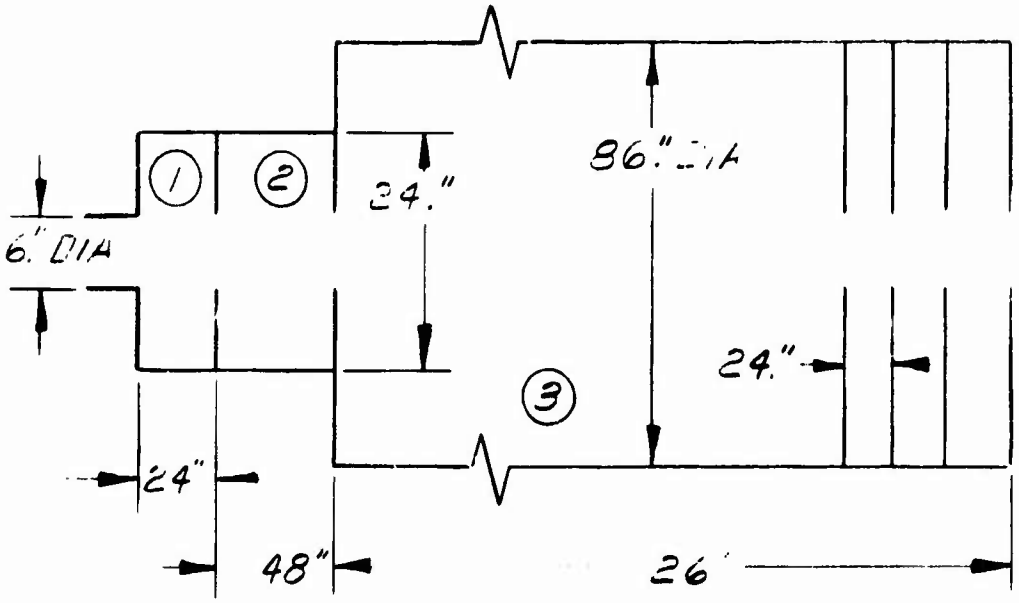

Figure 16. 155mm suppressor schematic.

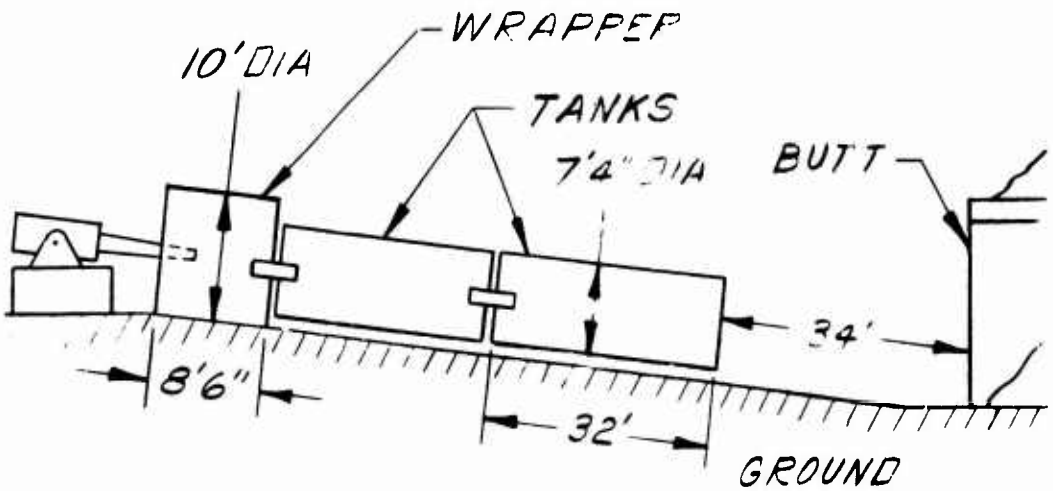

Figure 17. Simplified full scale suppressor.

motion of the cylinders, but did not provide an air tight seal between them. Thus, as tested, the simplified suppressor consisted of one high pressure chamber with a relatively large orifice and volume, followed by a 64 foot long cylindrical duct with no baffles.

Before the cylindrical portion was added, test firings were performed using the wrapper alone. The primary purpose of these lists was to determine if the wrapper could withstand the high muzzle pressures expected in the first chamber. Subsequent inspection of the wrapper should show no damage caused by the muzzle blast. Those who heard the blast emitted by the wrapper orifice said that the wrapper alone did not seem to have noticeably reduced the muzzle blast generated noise.

Figure 18 shows the relative spectrum levels as measured by Mr. D. Driscoll at the N.Y.S. Department of Environmental Conservation for the wrapper alone. A 105mm M68 tank gun was used in these tests. The peak sound pressure level at 1.5 miles was 107 db for a typical round. The solid line in thus figure represents the estimated unmuffled spectrum for a muzzle blast signal of the type $f(t) = h\left(1 - \frac{t}{\tau}\right) e^{-t/\tau}$. The wrapper noticeably reduces the level above 15 Hz, but has little effect on lower frequencies.

Figure 19 shows the relative spectrum as measured by Mr. Driscoll following the installation of the 64 foot long cylindrical section and a reduction in the down range wrapper orifice size from 20" to 6.5". The fundamental resonant frequency of cylindrical tank section is calculated to be 4 Hz. Other resonant frequencies would be expected at integer multiples of the fundamental, i.e., 8, 12, 16, 20, 25 Hz. The

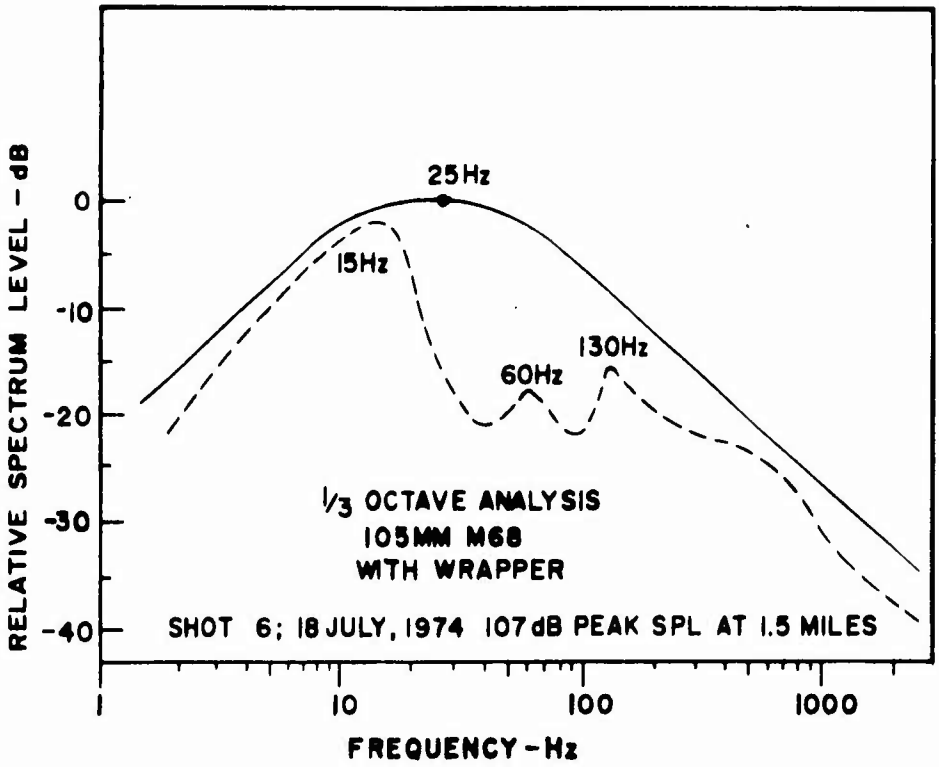

Figure 18. Relative spectrum level-wrapper.

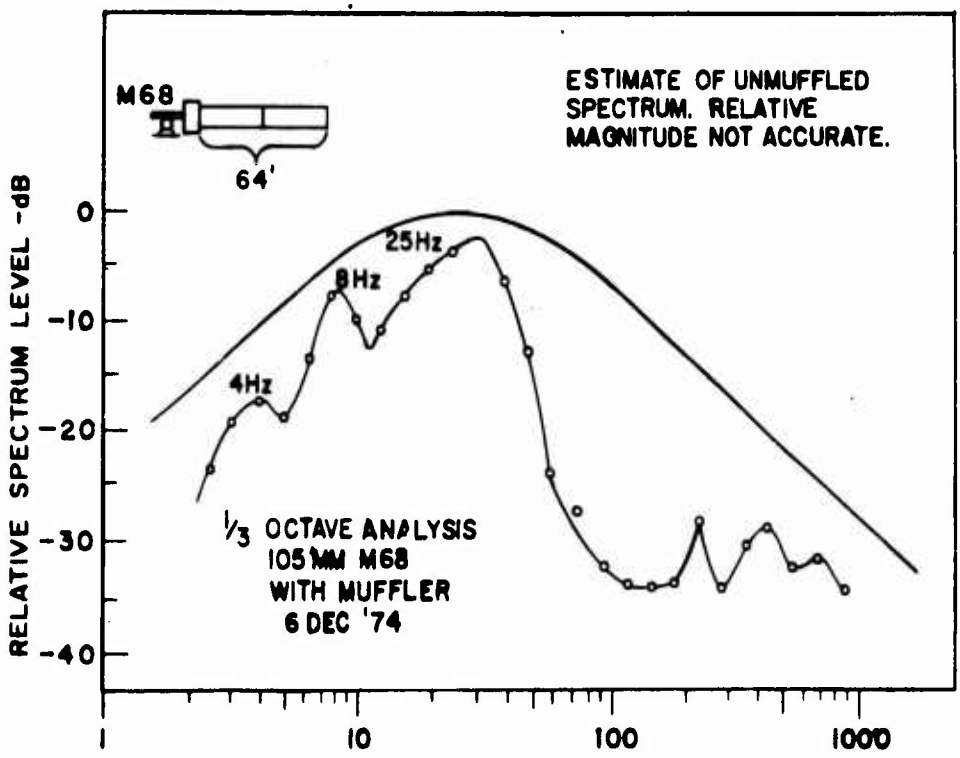

Figure 19. Relative spectrum level-simplified full scale design.

fundamental and the first harmonic are clearly evident in Figure 19. The closeness of the next 4 harmonics on a logarithmic plot may mask their individual presences. However, above 30 Hz there is a rapid reduction in level with increasing frequency to levels about 10 db below those obtained with the wrapper alone. This reduction, coupled with the somewhat more modest low frequency reductions introduced by the long, open-ended cylindrical section are undoubtedly the reason for the overall reduction recorded. The average of 6 rounds was found to be about 103 db (normalized to 1 mile) which is 7 db less than the average of the previous measurements for the wrapper alone. On this basis, Mr. Driscoll calculated the average value at the nearest residence would be 99 db. Actual measurements at the residence were 94.9 and 96.3 db, where the difference from the predicted value was attributed to atmospheric refraction.

Further evidence of the relative effectiveness of the various components of the suppressor is illustrated in Figures 20 and 21. Figure 20a is the trace of the pressure signal 4'5" above the ground, 16' 3 1/2" from the projectile flight path, and 59'5" from the wrapper exit which was recorded before the two 32' cylindrical tanks were put in place. The peak pressure received was 2 1/4 psi from the muzzle blast. Figure 20b shows the pressure signal recorded at the same location following the installation of the two tanks. The blast wave now has a peak value of 3/16 psi. Because of the length of the tanks, this

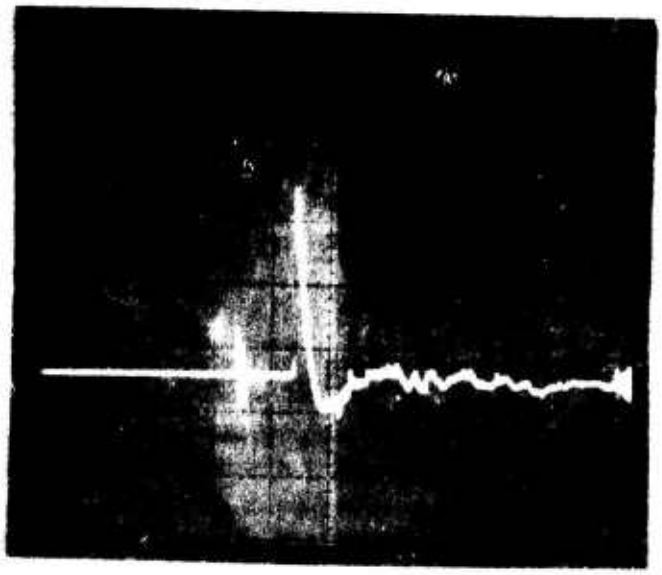

Figure 20a. Blast pressure-wrapper, RD 187.
SWEEP 20 MS/DIV, SENSITIVITY 3/4 PSI/DIV.

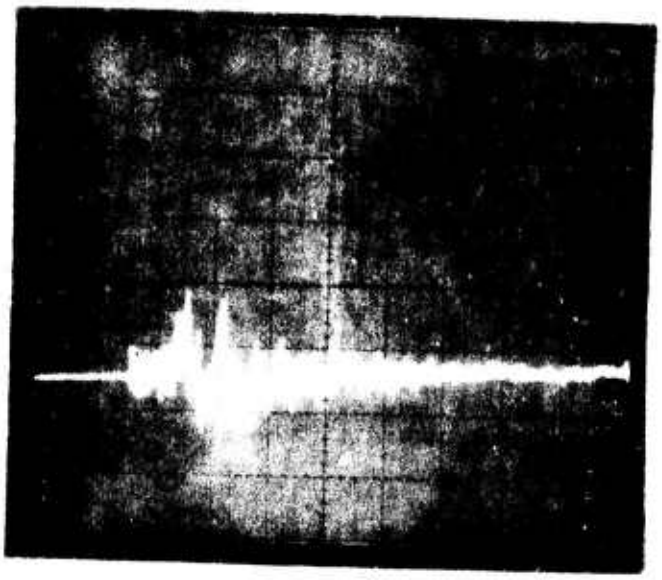

Figure 20b. Blast pressure-wrapper and tanks, RD 393.
SWEEP 50 MS/DIV, SENSITIVITY 1/8 PSI/DIV.

pressure occurs roughly 5' behind the mouth of the suppressor at the butt-end, i.e., "around the corner" from the exit where diffraction has the effect of reducing the blast intensity.

Pencil gages, located at the mouth of the butt-end tank and facing toward the wrapper, measured the maximum blast wave pressures which propagated through the tanks. These were found to be in the range 1 1/4 to 1 3/4 psi. They are lower than the typical values computed for proposed 155mm design, due probably to the relatively large volume of the wrapper, the length of the cylindrical tanks, and the difference in guns. These relatively small values are encouraging from a structural integrity point of view.

Figure 21a compares the pressure signals recorded at the top of the butt with wrapper and two tanks (upper trace) and a single 32' long tank open at both ends and no wrapper (lower trace). The wrapper orifice diameter had been reduced from 20" to 6.5" for these tests. Figure 21b shows the pressure traces measure 75' to the rear of the gun for the same two arrangements, wrapper plus two tanks (upper trace), single tank (lower trace). The attenuation of the blast wave caused by the wrapper and the addition of an extra tank is quite evident. The addition of downstream baffles at the butt-end would no doubt further improve the overall performance. The relatively low reflected pressures which occur there, roughly three psi, would make this appear to be feasible.

Thus, it appears that even the most rudimentary suppressor constructed along the lines of the design proposed in this report can produce substantial reductions in all but the lowest frequency components of the

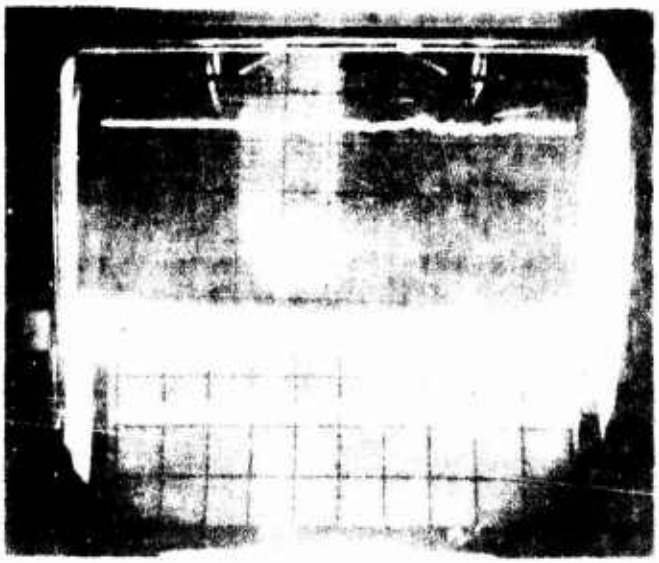

Figure 21a. Blast pressure on butt top-wrapper and tanks (upper), single tank (lower).

SWEEP 20 MS/DIV SENSITIVITY 1 PSI/DIV.

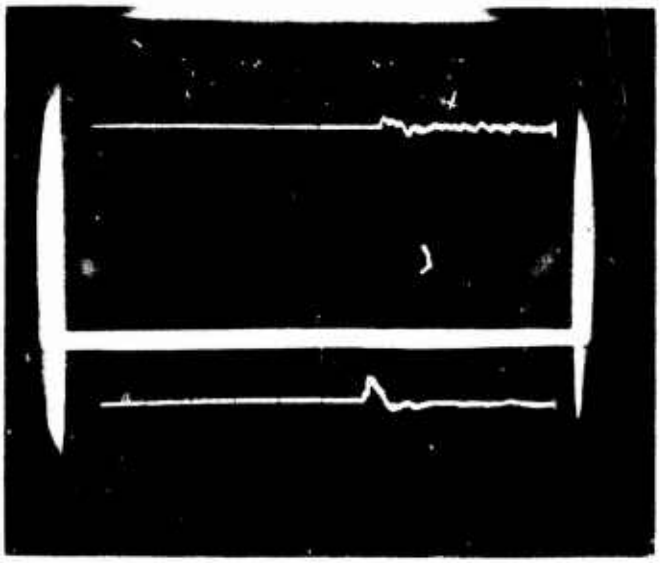

Figure 21b. Blast pressure at 75 ft-wrapper and tanks (upper), single tank (lower).

SWEEP 20 MS/DIV, SENSITIVITY 1 PSI/DIV.

muzzle blast. Even these lower frequencies are attenuated several db, contributing to the overall sound reduction. Further refinements, such as butt-end baffles, a wrapper to gun barrel seal, and piling earth over the cylindrical portion would certainly enhance the already creditable performance of this simple design.

VI. GENERAL CONCLUSIONS

1. The simulation of the non-steady impulsive discharge of a gun barrel through a two-dimensional model of a noise suppressor on the water table is proven to be an extremely useful technique for qualitatively ranking various proposed configurations.

2. A simple, one-dimensional shock wave analysis has been adapted to suppressor configurations which can be used by the designer to estimate the maximum pressure differences exerted on the silencer baffles by reflected shock waves.

3. A lumped-parameter analysis has been devised for the unsteady bulk flow of the discharged gas flow through the silencer following the passage of the initial shock wave.

4. Model tests on a silencer using the high-low pressure chamber concept indicate that this new design concept very effectively reduces the muzzle blast induced noise level.

5. The lumped-parameter predictions of the sound level reductions expected from the 20mm model suppressor were found to be good agreement with the measured attenuations in the range of the theory's validity.

6. The analysis of the proposed 155mm suppressor indicates that it will also effectively attenuate the muzzle blast noise.

7. The noise produced by the 155mm projectiles flight may still produce sound levels which are perceived by distance listeners. Whether this noise will be judged by the listener to be objectionable cannot be foretold.

8. The pressures which the small, high pressure, first-stage suppressor must withstand are quite large and for that reason the cost of constructing a long-lived, permanent installation capable of handling large caliber guns is considered to be quite high.

9. Tests with a simplified full-scale design show that substantial reductions in sound levels can be obtained using the concepts described in this report. Further reductions can certainly be obtained if the proposed suppressor design is fully implemented.

ACKNOWLEDGMENT

The author wishes to express his gratitude to Mr. D. A. Driscoll of the New York State Department of Environmental Conservation, Bureau of Noise Control, for his generous assistance and cooperation throughout the period of this project. Mr. G. Shanley, Mortar and Recoilless Rifle Division, is also recognized for his invaluable contribution to the design and fabrication of the 20mm and modified full scale suppressors.

DEPARTMENT OF THE ARMY
WATERVLIET ARSENAL
WATERVLIET, N. Y. 12189

OFFICIAL BUSINESS
PENALTY FOR PRIVATE USE. $300

SARWV-RDT-TP

POSTAGE AND FEES PAID
DEPARTMENT OF THE ARMY
DOD-314

THIRD CLASS

Commander
Defense Documentation Center
ATTN: DDC-TCA
Cameron Station
Alexandria, Va. 22314